UNIVERSITÀ DEGLI STUDI DI PADOVA

DIPARTIMENTO DI BIOLOGIA

Corso di Laurea magistrale in Molecular Biology

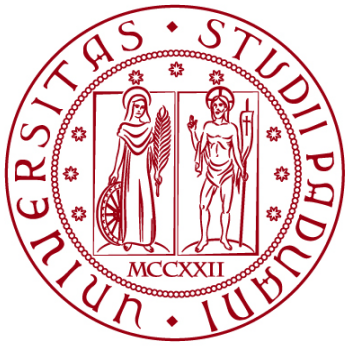

TESI DI LAUREA

Evaluating the effect of a new inhibitor of USP14 in a Drosophila model of ALS

Relatore: Prof.ssa Elena Ziviani
Dipartimento di Biologia, Università degli Studi di Padova

Laureanda: Sonia Luciano

ANNO ACCADEMICO 2024/2025

TABLE OF CONTENTS

ABSTRACT

Protein and organelle homeostasis (proteostasis) comprises the cellular mechanisms responsible for maintaining protein and organelle stability, which is essential for cell physiology and proper function. Two primary quality control systems oversee protein and organelle turnover and are in charge of degrading damaged proteins and organelles: the ubiquitin-proteasome system (UPS) and the autophagy-lysosome system. Both processes share a common molecular tag, ubiquitination, which targets the substrate for degradation. Ubiquitination is a post-translational modification that is attached to substrates by specific E3-ubiquitin ligases. This process is reversible thanks to the action of deubiquitinating enzymes (DUBs), which can hydrolyse the ubiquitin bonds, and trim ubiquitination moieties from substrates.

Proteostasis can be compromised during ageing and in many neurodegenerative diseases, like Amyotrophic Lateral Sclerosis (ALS). Thus, approaches that enhance cellular proteostasis may benefit human diseases like ALS.

We can enhance proteostasis by acting on DUBs: inhibiting specific DUBs stabilizes ubiquitination, and enhance the activity of the UPS and autophagy, thus promoting cellular proteostasis.

In this project, we explore the potential beneficial effect of inhibiting USP14, a proteasome-associated DUB that negatively regulates both autophagy and the UPS. Using a *Drosophila melanogaster* model of ALS, we aim to determine whether enhancing proteostasis by USP14 inhibition can ameliorate the disease phenotype of these flies.

1. INTRODUCTION

1.1 Amyotrophic Lateral Sclerosis

Amyotrophic Lateral Sclerosis (ALS) is an adult-onset neurodegenerative disease, characterized by the loss of both lower motor neurons, at the level of the spinal cord and brainstem, and upper motor neurons in the motor cortex. This loss brings to muscle weakness, atrophy, spasticity and in most cases to respiratory failure.

ALS is a progressive disease since motor neurons degeneration spreads gradually, and usually, life expectancy is between 2 to 5 years from the symptoms onset. (Masrori & Van Damme, 2020)

Symptoms appear when axonal connections fail, which occurs when the axon retracts, and lower motor neurons or muscles are denervated. In the early stages, this retraction is counterbalanced by collateral reinnervation from axons of neurons that seem to be more resistant to degeneration. However, as the disease advances, even these resistant neurons are affected, leading to the failure of this compensatory mechanism. (Robberecht & Philips, 2013)

Additional non-motor symptoms can be registered in 50% of patients: in 35-40% of cases mild behavioural and cognitive changes are recorded, while in 10-15% of cases it is possible to diagnose Frontal Temporal Dementia (FTD), which is characterized by the degeneration of the frontal and anterior temporal lobes. FTD result in behavioural changes, language impairment and problems in executive functioning. (Robberecht & Philips, 2013)

ALS is classified into two categories: familial ALS (fALS) and sporadic ALS (sALS). fALS is a hereditary form and constitutes 10% of cases, while sALS is the prevalent form and it is attributed to patients without a familial history. There are no clinical features that allow to reliably distinguish these two categories. (Robberecht & Philips, 2013)

At genetic levels, ALS is a heterogeneous disease, with more than 20 genes involved. The most common genetic causes of the disease are mutations in superoxide dismutase 1 (*SOD1*), fused in sarcoma (*FUS*), TAR DNA-binding protein 43 (*TARDBP*), TANK-binding kinase 1 (*TBK1*), and hexanucleotide expansions in chromosome 9 open reading frame 72 (*C9orf72*).

The defining neuropathological characteristic of ALS is the presence of cytoplasmic aggregates of TDP-43, a protein encoded by the *TARDBP* gene, found in over 95%

of cases. These TDP-43 inclusions occur not only in individuals with *TARDBP* mutations but also in those with *C9orf72* expansions or *TBK1* mutations.
In addition, other proteins, such as SOD1 and FUS, form aggregates in ALS cases linked to *SOD1* and *FUS* mutations, respectively. Patients with *C9orf72* hexanucleotide repeat expansions also display accumulations of dipeptide repeat proteins, which result from the translation of GGGGCC repeats within a non-coding region of the gene. (Masrori & Van Damme, 2020)

1.2 *In vivo* models of ALS

Various *in vivo* models have been developed to explore the intricate mechanisms underlying ALS. Regarding TDP-43, research has been conducted on different animal models.
In zebrafish (*Danio rerio*), TDP-43 mutations result in severe motor impairments, including axon shortening, locomotor deficiencies, a reduced lifespan, paralysis, neurodegeneration, and increased oxidative stress. (Gois et al., 2020)
Mice models have revealed cortical neuron damage, mitochondrial dysfunction, motor deficits, neuronal loss, axonal degeneration, and the deterioration of neuromuscular junctions. (Gois et al., 2020)
Research on *Drosophila melanogaster* has shown a reduction in voltage-gated calcium channels, neuromuscular junction damage, impaired larval locomotion, and age-related motor dysfunction in adults. Additional findings include abnormal mRNA and TDP-43 protein levels, axonal transport defects, and a degenerative phenotype characterized by a shortened lifespan (Gois et al., 2020).
Many studies have used the Drosophila model and its *TDP-43* orthologous, TAR DNA-binding protein-43 homolog (*TBPH*), to investigate the role of this gene in the pathogenesis of ALS, assessing whether it results from a gain or loss of protein function.
Overexpression of wild-type or mutant human TDP-43 leads to a reduction in lifespan, impairment in motor function, cytoplasmic toxic aggregation and eclosion failure. Similar phenotypes are obtained through overexpression of *TBPH* gene. (Liguori et al., 2021).
Moreover, loss of TBPH induces a pathological phenotype, with defective motor behaviour, lifespan reduction and eclosion defects.

Interestingly, these results show that positive or negative deviation from a threshold expression of *TBPH* might induce ALS-like features in Drosophila. (Liguori et al., 2021)

1.3 TDP-43 accumulation in ALS

In 95% of ALS patients an accumulation of TDP-43 protein is detected. This accumulation is not only common when *TARDBP* is mutated, but also in patients with *TBK1* mutation or with hexanucleotide expansions in *C9orf72*. (Masrori & Van Damme, 2020)

TDP-43 is a ubiquitous expressed DNA/RNA binding protein, which contains two RNA recognition motifs: a nuclear localization signalling (NLS) and a nuclear export signalling (NES), which regulate the shuttling of the protein between nucleus and cytoplasm. It also presents a glycine-rich C-terminus, which has a role in mediating protein-protein interaction (FIGURE 1). (X. Wang et al., 2024)

In normal conditions, TDP-43 is predominantly situated in the nucleus where it participates in transcription and RNA processing. Around 30% of this protein is found in the cytoplasm, where it is implicated in the regulation of RNA spatial distribution, and it localizes in P-bodies, RNA transport granules and stress granules. (Baldwin et al., 2016)

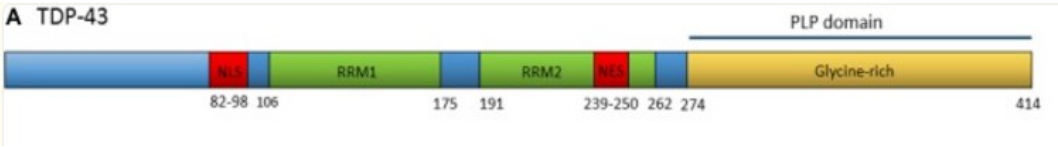

Figure 1. Domain structures of TDP-43*. TDP-43 is constituted by two RNA recognition motives, RRM1 and RRM2 (in green); a nuclear localization signal (NLS), a nuclear export signal, (NES), (both in red), which mediates the shuttling of the protein between the nucleus and the cytoplasm; and a Glycine-rich domain, the Prion-like protein (PLP) domain (in yellow), which mediates protein-protein interaction. (Mejzini et al., 2019)*

In ALS-affected tissues, the truncated form of TDP-43 aggregates in the cytoplasm, while, at the level of the nucleus, the protein is gradually cleared. The exact mechanism of the aggregates' formation is still unknown.

Most forms of truncated proteins are the N-terminal truncated, C-terminal fragment, CTF35 and CTF25, which are generated by the proteolytic cleavage via caspase. (Scotter et al., 2015)

Post-translational modifications, such as ubiquitination, phosphorylation, acetylation and SUMOylation, accumulate at the level of these aggregates and cause functional toxicity. (Suk & Rousseaux, 2020)

Phosphorylation of TDP-43 predominantly occurs at serine 409 and 410 (S409/410), with most phosphorylation sites located in the glycine-rich C-terminal domain (CTD). This modification influences subcellular localization, promoting increased nucleolar and mitochondrial localization. Additionally, TDP-43 ubiquitination plays a key role in protein aggregation and inflammatory responses. Acetylation, on the other hand, impairs the ability of TDP-43 to bind and splice RNA, further enhancing aggregate formation. (X. Wang et al., 2024)

Abnormal accumulation of TDP-43 results in dysregulation of RNA metabolism, loss of TDP-43 nuclear function and acquisition of cytoplasmic toxicity. (Mejzini et al., 2019)

Recent studies have demonstrated that in ALS-affected tissues TDP-43 not only accumulate at the level of cytoplasm, but also specifically within mitochondria.

Protein accumulation inside the organelle causes an increase in the production of radical oxygen species (ROS) and a decrease in mitochondrial membrane potential. These events determine the opening of the permeability transition pore (mPTP), resulting in the release of mitochondrial DNA (mtDNA) into the cytoplasm. mtDNA accumulation in the cytoplasm activates the cGAS/STING pathway that promotes the innate immune activation (FIGURE 2). (Suk & Rousseaux, 2020)

In a nutshell, cGAS binds mtDNA and goes through a conformational change, which activates the catalytic domain and induces the production of cyclic GMP-AMP (cGAMP) from ATP and GTP. cGAMP binds STING and activates it. At this point, STING can bind a kinase TBK1, which phosphorylates the transcription factor IRF3, which then can enter the nucleus. At the same time, STING phosphorylates Ik-β, a family of NF-kβ inhibitors, which is degraded by the ubiquitin-proteasome pathway. NF-kβ enters the nucleus and, together with IRF3, promotes the expression of interferons and inflammatory cytokines(Chen et al., 2016)

At the level of motor neurons, the expression of these molecules causes a decrease of motor neuron function and neuronal loss.

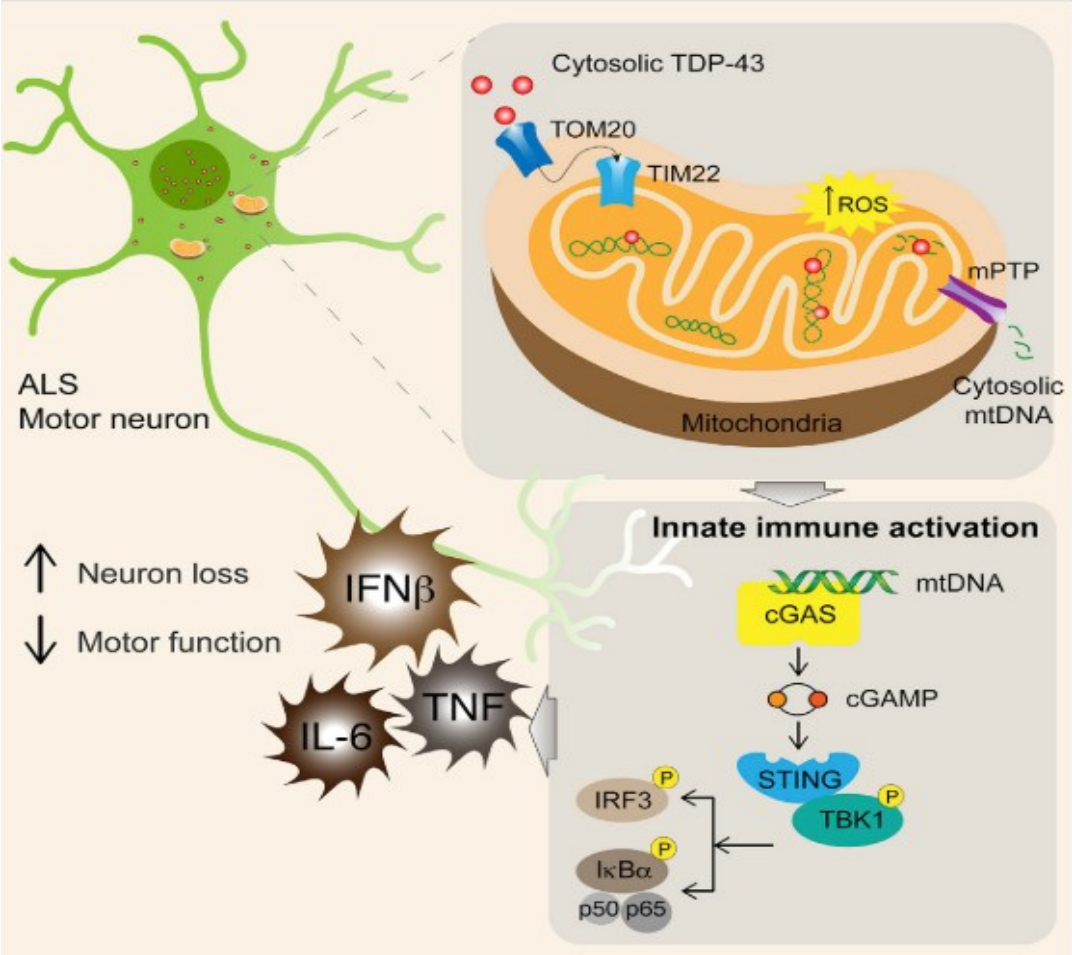

Figure 2. TDP-43 accumulation inside mitochondria triggers mitochondrial DNA release and activation of the GAS/STING pathway. *TDP-43 accumulation inside mitochondria causes the increase of ROS production and decrease in mitochondrial membrane potential, which leads to the release of mtDNA through the* permeability transition pore *(mPTP). In the cytoplasm, mtDNA accumulation activates the cGAS/STING pathway by binding cGAS, and determines the activation of innate immunity, which causes the release of inflammatory cytokines and interferons through the activation of IRF3 and NF- kβ. In motor neurons, the release of interferons and inflammatory cytokines causes neuron loss and a decrease of motor function. (Yu et al., 2020)*

The accumulation of dysfunctional protein aggregates is a hallmark of neurodegenerative diseases. In ALS, TDP-43 aggregates disrupt protein homeostasis and induce cellular stress. This stress interferes with essential cellular functions, including intracellular transport, cytoskeletal integrity, and mitochondrial function, ultimately leading to axonal retraction and cell death. (Robberecht & Philips, 2013)

Thus, preserving proteostasis by preventing TDP-43 misfolding and aggregation, and/or enhancing its clearance could represent a promising therapeutic strategy for ALS.

1.4 Protein and organelle homeostasis: role of the UPS and Autophagy

Protein and organelle homeostasis (proteostasis) refers to the network of cellular processes involved in the maintenance of protein stability and correct function with the aim of avoiding unwanted accumulation of dysfunctional proteins and/or organelles. This process includes mechanisms for proteins folding, transport and degradation, and it is essential for organelle biogenesis, cellular metabolism and adaptation to stress conditions.

Proteostasis is often compromised during aging and in many neurodegenerative diseases, including Amyotrophic Lateral Sclerosis (ALS); thus, proteostasis is becoming a potential target of increasing interest for human diseases.

The main systems involved in the maintenance of proteostasis are molecular chaperons, the ubiquitin-proteosome system (UPS) and the autophagy-lysosome system.

Molecular chaperones are necessary for *de novo* proteins folding, assembly and disassembly and transport across membranes. In this way molecular chaperones ensure proper protein folding and prevent aggregate formation.

When chaperones are unable to bend aberrant proteins into their native form, these proteins are targeted for degradation.

(Yu et al., 2020)

The two main degradative systems of the cell are the ubiquitin-proteosome system (UPS) and the autophagy-lysosome system. UPS is the main proteolytic system responsible for the degradation of small and short-lived proteins that are damaged or misfolded. The recognition of targeting proteins is mediated by ubiquitination which involves three types of enzymes: the ubiquitin-activating enzyme, E1; the ubiquitin-conjugating enzyme, E2; and the ubiquitin ligase, E3. (Lambert-Smith et al., 2022)

Conjugation of ubiquitin (Ub) starts with the ATP-dependent activation of the C-terminal glycine residue, mediated by E1. Activated Ub is handed to E2 enzyme, which cooperates with E3 ubiquitin ligase and promotes the transfer of Ub at the level of a lysine residue of the target protein. Additional Ub are added by the same

cascade of events, creating a chain. Polyubiquitinated substrate is then transferred to the 26S proteasome to be degraded. (Lambert-Smith et al., 2022)

The 26s proteasome is an ATP-dependent protease, made up of two subcomplexes, the 20s core particle and the 19s regulatory particle, which is localized at one or both ends of the 20s particle. In the core particles are localized three β-type subunits, β1, β2, and β5, which possess the catalytic activities, respectively caspase-like, trypsin-like and chymotrypsin-like. These subunits digest the proteins into peptides of 2-24 amino acids, ensuring correct degradation and providing a source of amino acid (Figure 3). (Kaushik & Cuervo, 2015)

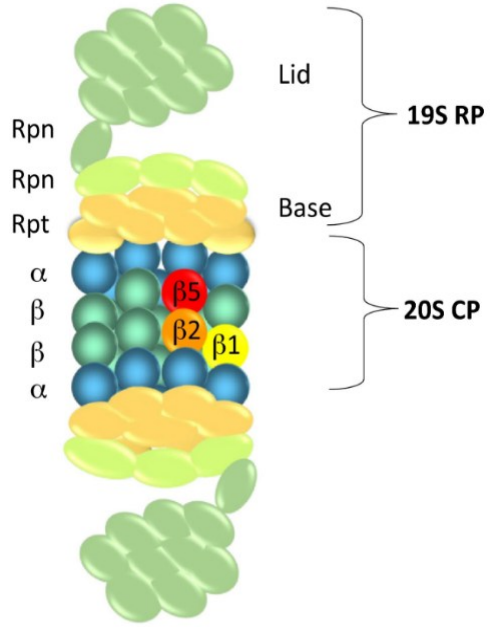

Figure 3. Proteasome structure. *Schematic representation of the 26s proteasome with its main subunits, the 20s core particle and the 19s regulatory particles, which are localized at both ends of the 20s core particle. At the level of the core particle are localized the three catalytic subunits,* β1, β2, *and* β5 (*represented in yellow, orange and red, respectively), which possess the catalytic activity, caspase-like, trypsin-like and chymotrypsin-like, respectively.* (Myeku & Duff, 2018)

Autophagy is responsible for the degradation of protein complexes, organelles and aggregates of higher dimensions; substrates are delivered to lysosome to be degraded. Three different types of autophagy are known: macro-autophagy,

micro-autophagy and chaperone-mediated autophagy, which are distinguished by the way in which cargo is delivered to the lysosome. (Gatica et al., 2018)

In macro-autophagy, the cargo is delivered across a double membrane-bound structure, called autophagosome, which fuses with the lysosome to form the autolysosome. In micro-autophagy the lysosome directly engulfs the cargo trough a membrane invagination. In chaperon-mediated autophagy, targeted proteins are driven to the lysosomal membrane by a complex of chaperone molecules, which is recognized by a lysosomal membrane receptor, the lysosomal-associated membrane protein 2A (LAMP-2A) (Figure 4). (Gatica et al., 2018)

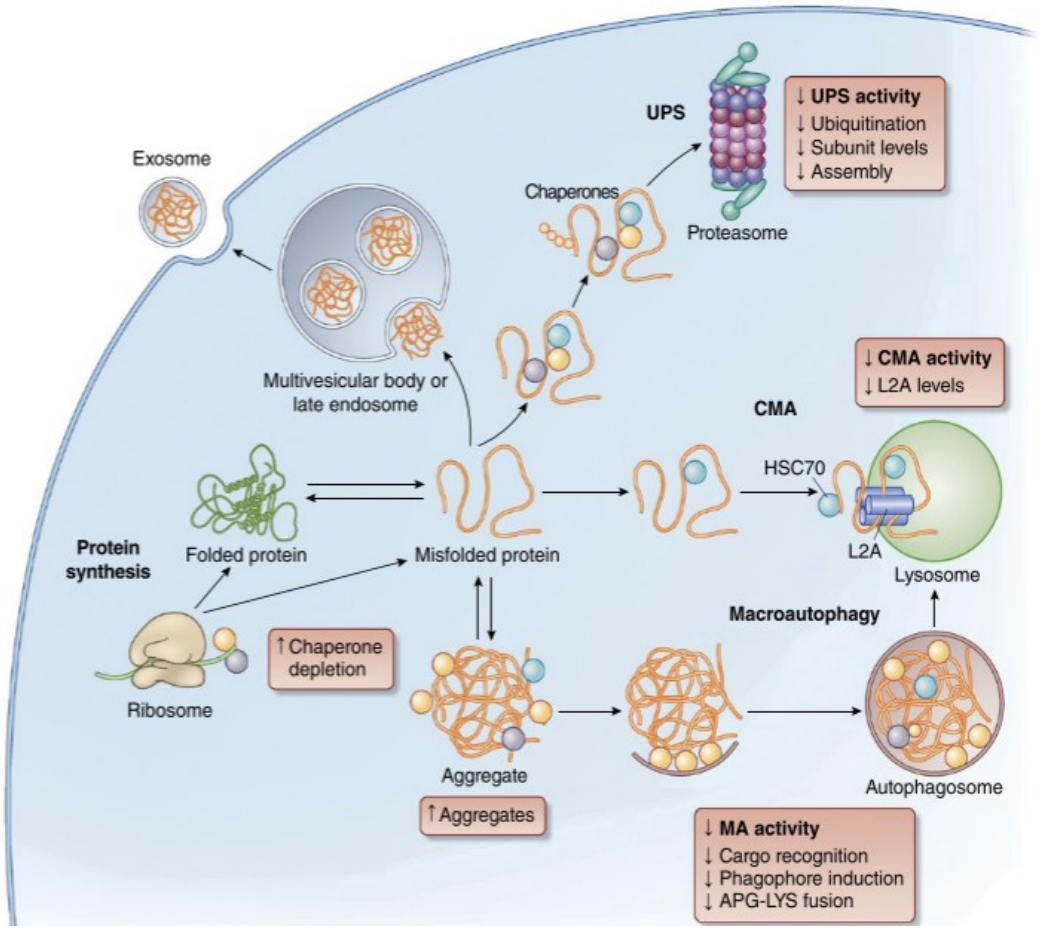

FUGURE 4. Maintenance of protein homeostasis. *The main systems involved in the maintenance of protein homeostasis are molecular chaperons, the ubiquitin-proteosome system (UPS) and autophagy. Molecular chaperones promote de novo folding of synthetized proteins, preventing aggregate formation.*

When chaperones are unable to bend aberrant proteins into their native form, misfolded proteins are targeted for degradation. Small and short-lived proteins are processed by the UPS while higher dimension proteins and organelles are degraded by autophagy. Depending on how proteins are delivered to the lysosome in

autophagy, we can distinguish three mechanisms: the chaperone-mediated autophagy, in which chaperones drive proteins to the lysosome, the micro-autophagy where lysosomes engulf the proteins directly and the macro-autophagy, in which we have the formation of an autophagosome that englobes the content and fuses with the lysosome. (Kaushik & Cuervo, 2015)

Macro-autophagy is the major type of autophagy. It is subdivided into selective autophagy, which degrades damaged organelles, and non-selective or bulk autophagy, which is induced by nutrient deprivation. Selective autophagy participates in the degradation of cellular organelles, like mitochondria, peroxisomes and the endoplasmic reticulum (ER). The selective pathway for mitochondria degradation, called mitophagy, is a fundamental process for cellular quality control. Alterations in this process have been associated with many pathologies, including neurodegenerative diseases. (Gatica et al., 2018)

Mitochondria perform multiple metabolic functions and regulate cellular apoptosis. Therefore, damage in these organelles can compromise the metabolic homeostasis. Moreover, disruption of oxidative phosphorylation (OxPhos) in damaged mitochondria can lead to an excessive production of reactive oxygen species (ROS). (Gatica et al., 2018)

For these reasons, the maintenance of quantity and quality of mitochondria is crucial and damaged or superfluous ones must be degraded. The main role in preserving mitochondria integrity is played by mitophagy, which cooperates with the ubiquitin-proteasome system (UPS) to ensure mitochondrial homeostasis. (Gatica et al., 2018)

Mitophagy is a complex system that requires multiple signalling. Three main steps are necessary: (1) fragmentation of the mitochondrial network (mitochondrial fission) to obtain a suitable dimension that can be engulfed, (2) priming to allow recognition from the autophagic system and (3) engulfment of mitochondria by the autophagosome. (Figure 5)

Mitochondrial fission is catalysed by the GTPase dynamin-related protein 1 (Dpr1), which is recruited from the cytosol to specific mitochondrial sites by several adaptors localized at the level of the organelle surface. The oligomerization of Drp1 and the subsequent GTP hydrolysis results in mitochondrial membrane constriction at the fission site. (Yoo & Jung, 2018)

Targeted mitochondria are recognized by autophagosome through LC3 adapter in a ubiquitin-dependent or independent way.

In the ubiquitin-dependent pathway, the first step is the ubiquitination of proteins that are localized on the mitochondrial surface, and subsequent recognition by LC3 adaptors.

PINK1/Parkin is the best-characterized ubiquitin-dependent mitophagy pathway. Parkin is an E3-ubiquitin ligase and PINK1 is a mitochondrial serine/threonine-protein kinase; under normal conditions PINK1 is imported into mitochondria through the TIM/TOM translocase complex, cleaved by a protease located in the mitochondrial inner membrane, the presenilin-associated rhomboid-like (PARL), and rapidly degraded by the UPS.

Depolarization of the mitochondrial membrane resulting from mitochondrial damage affects the TIM/TOM translocase complex, thus leading to the accumulation of PINK1 on the mitochondrial surface. On the mitochondria, PINK1 phosphorylates ubiquitin and the E3-ubiquitin ligase Parkin on serine 65. PINK1-dependent phosphorylation of Parkin activates Parkin and promotes its translocation from the cytosol to the mitochondria. On mitochondria, Parkin poly-ubiquitinates a subset of mitochondrial resident proteins, which are subsequently detected by ubiquitin-binding proteins such as p62, optineurin (OPTN), Tax1-binding protein 1 (TAX1BP1), NRB1, and NDP52. These proteins contain an LC3-binding motif, which allows them to work as a bridge between ubiquitinated proteins on the mitochondrial surface and the autophagic protein LC3, major component of the forming autophagosome (Figure 5). (Yoo & Jung, 2018)

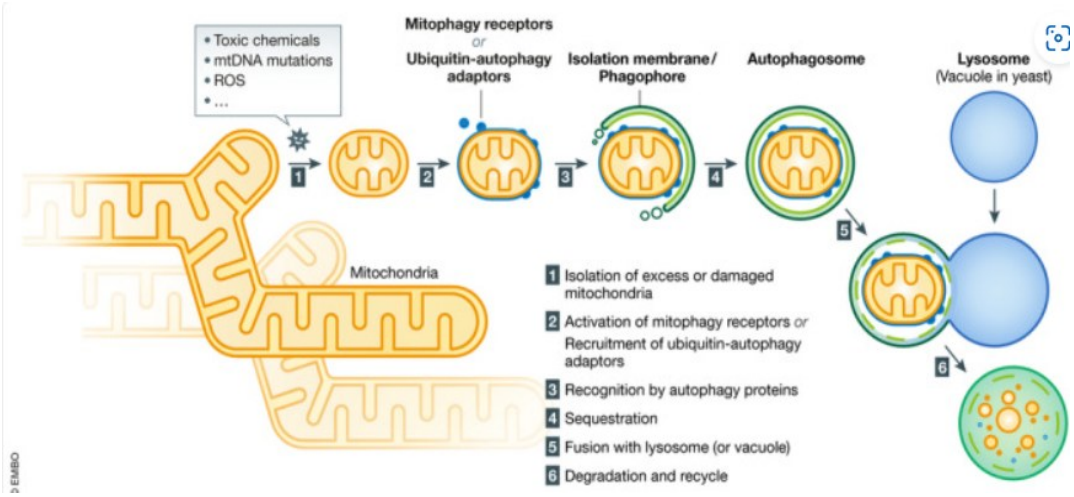

Figure 5. The main steps involved in mitophagy*. (1) Intra- and extracellular signals drive the isolation of excess or damaged mitochondria through the fragmentation*

of tubular networks. (2) mitophagy receptor or ubiquitin-autophagy adaptors are recruited at the level of mitochondrial membrane and confer selectivity for degradation. (3) Isolation membrane, or phagophore, is formed around the targeted mitochondria. (4) mitochondria are enclosed inside the autophagosome. (5) Autophagosome is fused with the catalytic component, the lysosome. (6) lysosomal hydrolases degrade the mitochondria inside the autophagosome, and the content is recycled. (Onishi et al., 2021)

In recent years, numerous studies have highlighted a strong connection between the ubiquitin-proteasome system (UPS) and autophagy with many diseases. These pathways play a critical role in neurodegenerative disorders, where defects in the mechanisms responsible for removing unfolded or aggregated proteins/organelles from the cytoplasm of neurons and glial cells are commonly observed.

1.4.1 Deubiquitinating enzymes (DUBs)

A common signature of neurodegenerative diseases is the aberrant accumulation of neurotoxic proteins at the levels of the central nervous system, not only due to their overproduction but also to improper degradation caused mainly by the dysfunction of the two principal protein quality control systems, the ubiquitin-proteasome system (UPS) and the autophagic pathway.

The most remarkable similarity between the two degradation systems is the labelling of target proteins with ubiquitin to allow the recognition and facilitate the degradation. Ubiquitination is a reversible process mediated by a cascade of ubiquitinating enzymes and counter-regulated by the deubiquitinating enzymes (DUBs), which can hydrolase the ubiquitin binding and avoid protein degradation.

Once proteins are marked for degradation, the Ubiquitin E3 ligases promote the formation of a covalent isopeptide bond between the C-terminus of the ubiquitin and a lysine residue on the substrate; DUBs can cleave this isopeptide bond and generate free ubiquitin. In this way, they antagonize the degradation of the substrate (Liu et al., 2022)

The involvement of DUBs in the regulation of these degradative processes makes them a compelling target for therapeutic development in neurodegenerative diseases.

In mammals, around 100 DUBs have been identified that can be divided into two main classes, cysteine proteases and metalloproteases. Metalloproteases only contain a family, the JAB1/MPN/MOV34. The cysteine proteases are, instead, the most abundant and can be subdivided into six families: the ubiquitin-specific proteases (USPs), the ubiquitin C-terminal hydrolases (UCHs), the ovarian tumour proteases (OTUs), Machado–Josephin domain (MJD), K48 polyubiquitin-specific MINDY domain families, and the zinc finger with UFM1-specific peptidase domain protein (ZUFSP/ZUP1). The USP class is the largest one and contains 58 members in the human genome. They are characterized by a hand-like structure with three domains: the palm, the thumb and the fingers. The thumb and the palm contain the catalytic domain, while the fingers stabilize the interaction with distal ubiquitin on substrates. (Snyder & Silva, 2021)

1.5 Ubiquitin-specific protease 14 (USP14)

Ubiquitin-specific protease 14 (USP14) is a proteasome-associated DUB which belongs to the ubiquitin-specific processing (UBP) family of proteases. This protein is located in the cytoplasm and cleaves the ubiquitin chain from ubiquitin-fused precursors and ubiquitinated proteins. The dysregulation of USP14 is common in many neurodegenerative diseases and therefore is acquiring higher interest as a therapeutic target.

In humans, the full-length USP14 comprises 494 amino acids and it is organized into two domains, a N-terminal ubiquitin-like domain, which is involved in the regulation of proteasomal activity, and a C-terminal catalytic USP domain, responsible for its deubiquitinating enzymatic activity. (F. Wang et al., 2022)

The catalytic domain displays a right-hand structure, characteristic of the USP family, with three domains: the palm, the thumb and the fingers, which constitute the ubiquitin-binding surface.

The thumb contains six α helices (α1- α6) and a short β strand (β1), the palm consists of three α helices (α7- α9), one short β strand (β9), a central six-stranded β sheet (β5, β8, β10– β13) and several surface loops. The finger subdomain comprises five β strand (β2– β4, β6, β7).

Moreover, two surface loops, named blocking loop 1 and 2 (BL1 and BL2), are localized above the binding pocket for ubiquitin and partially fill it: in this way, they

block the access of ubiquitin to the active site and maintain USP14 in a basal autoinhibitory state (Figure 6). (Hu et al., 2005)

Activation of USP14 is mediated by the interaction with the 26S proteasome through the displacement of BL1 and BL2 loops.

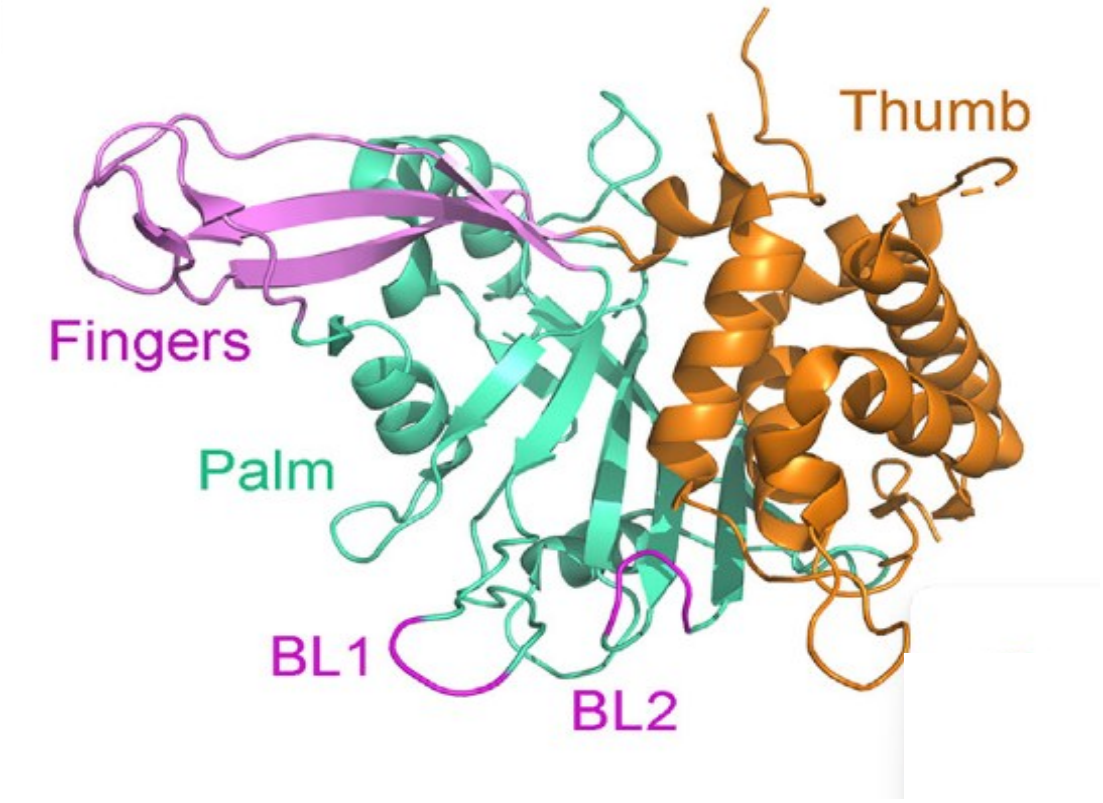

Figure 6. USP14 catalytic domain crystal structure*. The catalytic subunit shows a hand-right structure consisting of three domains: the thumb (in orange), the palm (in cyan) and the fingers (in magnet), which form the active site where ubiquitin is bound and degraded. BL1 and BL2 surface loops are represented in magnet, and they are responsible for the autoinhibitory function of USP14 due to their occupancy of the active site that avoids ubiquitin binding. (F. Wang et al., 2022)*

The activity of USP14 helps preventing stalling of ubiquitinated proteins on the 26S proteasome, acting as a timing mechanism that limits the available time for substrate hydrolysis and facilitating the release of the substrate without degradation. (Kim & Goldberg, 2017)

In addition to its catalytic role, USP14 is also involved in the allosteric regulation of the proteasome function, as it can both activate and inhibit multiple steps in Ub-conjugate degradation. Indeed, in the absence of a substrate, USP14 maintains the

26S proteasome in a quiescent state. When it binds an Ub-conjugated substrate, USP14 activates the proteasome degradative function by promoting ATP hydrolysis and enhancing substrate entrance into the core particle. (Kim & Goldberg, 2017)

USP14 is also involved in the regulation of autophagy, through the control of K63 ubiquitination of Beclin1. K63 ubiquitination of Beclin1 promotes its interaction with Atg14L and UVRAG, two important regulators of Vps34, which can phosphorylate phosphatidylinositol (PI) to produce phosphatidylinositol 3-phosphate (PtdIns), a key signal molecule for the induction of autophagosome formation. Since Atg14L and UVRAG enhance the activity of the Vps34 complex to mediate autophagy induction and autophagosome maturation, respectively, USP14-mediated K63 deubiquitination may not only regulate autophagy initiation through Atg14L complexes but also contribute to autophagosome maturation by modulating the UVRAG-containing Vps34 complex. (Xu et al., 2016)

Considering that USP14 regulates both proteasomal and autophagic degradation, inhibiting this enzyme provides a strategy to enhance these processes and improve proteostasis, which represents a potential therapeutic strategy in neurodegeneration. (Chakraborty et al., 2018), (Lee et al., 2010)

1.5.1 USP14 inhibition

Dysregulation of USP14 is highly involved in many pathological conditions, like cancer, neurodegenerative disease and viral infection, which is why identifying new inhibitors targeting USP14 is becoming an active field in research.
IU1 is the first specific USP14 inhibitor discovered in 2010 by Finley and coworkers. IU1 inhibits USP14 by binding at the level of the thumb-palm groove of the catalytic domain, preventing in this way the interaction with the substrate.
The inhibitor does not affect ubiquitin signalling in proteasomes lacking USP14 and has no effect in inhibiting other human DUBs. Moreover, in the absence of the proteasome, USP14 results insensitive to IU1 inhibition, suggesting that it binds specifically to the activated form of USP14. The half-maximal inhibitory concentration (IC_{50}) of IU1 for USP14 is equal to 4-5μM. (Lee et al., 2010)

In addition to its effect on the proteasome activity, it was confirmed that IU1 treatment also enhances autophagy by stabilising K63 ubiquitination on Beclin1, thereby promoting its interaction with Atg14L and UVRAG. (Xu et al., 2016)
Moreover, a study performed in our laboratory in 2018 confirms the involvement of USP14 in the regulation of autophagy and also showed that USP14 genetic or pharmacological inhibition induces mitophagy. Importantly, *in vivo* inhibition of USP14 restores mitochondrial function and improves locomotor behaviour in Pink1/parkin KO flies modelling Parkinson's disease. (Chakraborty et al., 2018)
This study showed for the first time that regulating UPS activity, autophagy and mitochondrial clearance via USP14 inhibition can function as a therapeutic strategy to mitigate the accumulation of aberrant proteins and organelles in cells and the entire organism.

Accumulation of aberrant proteins is a common marker of neurodegenerative disease, mainly due to the dysfunction of the two principal degradative pathways, UPS and autophagy. The capability of USP14 to negatively control both these pathways makes this DUB a possible therapeutic target of increasing interest.
After the discovery of IU1 in 2010, many inhibitors have been developed with increasing specificity for USP14, like IU1-47, with an IC_{50} equal to 0,6µM (Y. Wang et al., 2018)
The use of these inhibitors to promote an increase in proteostasis can be considered an interesting research area in neurodegenerative disease, like Amyotrophic Lateral Sclerosis (ALS).
In ALS, TDP-43 is the primary component of aberrant aggregates. Its degradation is primarily performed by the UPS and autophagy pathways, with ubiquitin tagging, crucial for recognition and degradation, promoted by the E2 ubiquitin-conjugating enzyme UBE2E3 and the E3 ligases Parkin and RNF.
USP14 inhibits the ubiquitination process that drives TDP-43 degradation, and its overexpression leads to increased levels of TDP-43 protein. Accordingly, USP14 inhibitor IU1 has been shown to enhance TDP-43 ubiquitination and accelerate its degradation by enhancing the extent of ubiquitin modification. (Liu et al., 2022)

1.6 *Drosophila melanogaster* as a model organism.

The fruit fly *Drosophila melanogaster* is a model organism highly used to understand the genetic component and the cellular and molecular mechanisms of a wide field of diseases, like cancer and neurodegenerative diseases.
One of the main advantages of using this model is that fruit flies are cheap and easy to keep, and it is possible to maintain a high number of stocks, thereby facilitating high-throughput experiments.
The life cycle of Drosophila spans approximately 10 days. At 25°C, the embryo develops into the larval stage within about 21 hours. The first instar larvae progress to the second and third stages over two days. Third instar larvae continue feeding for several days before leaving the food source to undergo pupariation. During the pupal stage, histolysis occurs, in which larval organs degenerate and are replaced by adult organs. At 18°C, the developmental time doubles (Figure 7).

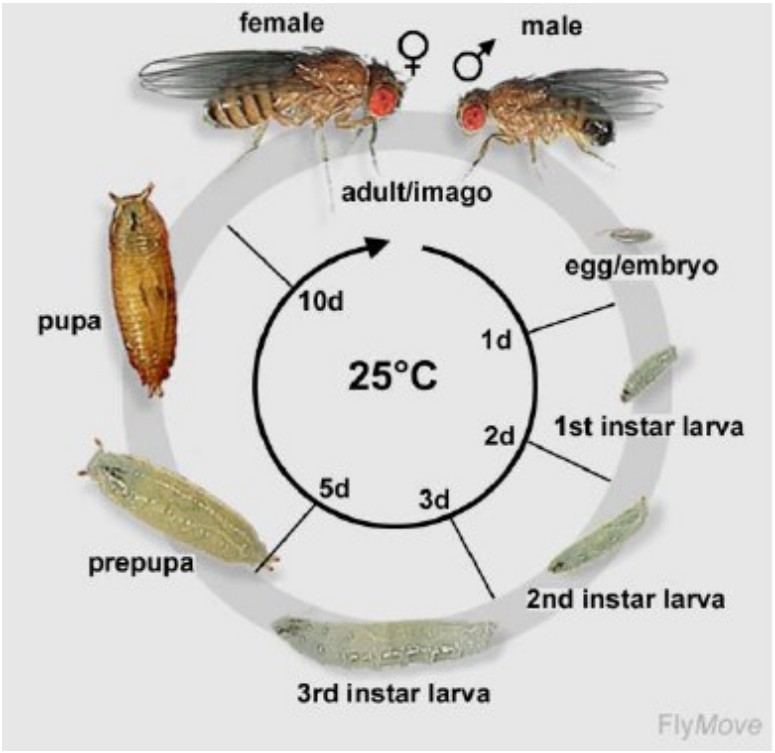

Figure 7. Drosophila melanogaster life cycle. *At 25°C, embryonic development lasts for 21h. 1st instar larva takes 2 days to moult into the second and then third larval stage. After one day, larvae leave food and, after the pupal stage, become adults. After 10 days from embryo development, adult flies emerge from pupal case.* (*A. Prokop-A Rough Guide to Drosophila Mating Schemes*, n.d.)

Drosophila is a diploid organism with two homologous chromosomes for each pair, meaning every gene is present in two copies. It has one pair of sex chromosomes, X/X in females or X/Y in males, and three pairs of autosomes.
For genetic crosses, males and females with the appropriate genotypes must be selected. Females are slightly larger and exhibit distinct dark stripes at the posterior tip of their abdomen, whereas males have merged stripes in this region and possess noticeable sex combs on their posterior legs.

Nowadays, Drosophila is highly used as an ALS model organism. What makes Drosophila an ideal model organism for Amyotrophic Lateral Sclerosis research is the ease of genetic manipulation, the high number of modalities to study disease progression and the fact that flies modelling ALS closely mimic human pathology in that they develop motor impairments, motor neuron degeneration, cellular inclusions, mitochondrial abnormalities, oxidative damage, and exhibit shorter lifespan. (Liguori et al., 2021)

Over the years, many genetic tools have been developed to study the role of genes in Drosophila, like the *UAS-GAL4* system.

GAL4 is a transcription factor from yeast, and it expresses genes downstream of the upstream activating sequences (UPS) enhancer element. This system does not exist in Drosophila endogenously and so it does not act on fly endogenous loci.

An important characteristic of this system is the possibility to regulate its expression in a temperature-dependent manner: it is enhanced by higher temperatures and decreased by lower ones (Figure 8).

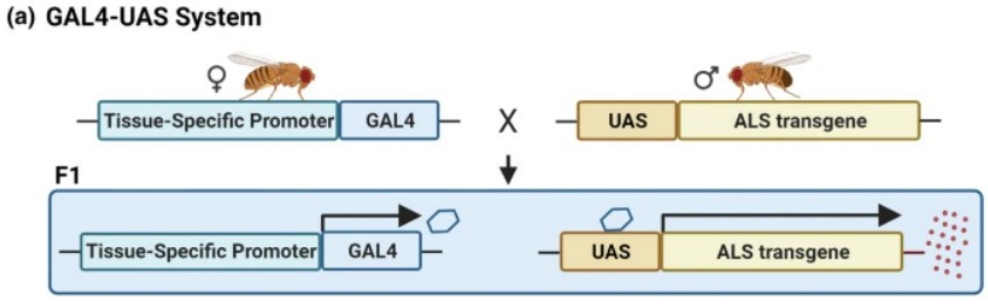

Figure 8. Schematic representation of the genetic system available for ectopic expression of human transgenes in Drosophila*. This model allows for targeted expression of a transgene within specific tissues through the GAL4-UAS system. It involves two distinct fly lines: one containing the yeast transcription factor GAL4*

under the control of a tissue-specific promoter, and another harbouring the transgene downstream of the UAS domain (the binding site for GAL4). Crossing these lines produces progeny (F1) in which the transgenic protein is expressed exclusively in tissues where GAL4 is active. (Liguori et al., 2021)

2. AIM OF THE STUDY

Amyotrophic Lateral Sclerosis (ALS) is an adult-onset neurodegenerative disease characterized by the degeneration of motor neurons activity, mainly due to the failure of axonal connection. This loss leads to muscle weakness, spasticity and, in most cases, failure of the respiratory system, which is the cause of death in most of the patients. ALS is a progressive disease since neurodegeneration spreads gradually, and the life expectancy is between 2 to 5 years from symptoms onset.

One of the main hallmarks of the disease is the formation of cytoplasmic toxic aggregates at the level of motor neurons, of which the main component is TDP-43 protein.

TDP-43 is a ubiquitously expressed DNA-RNA binding protein, which can normally shuttle between nucleus and cytoplasm. However, under pathological conditions, it accumulates in the cytoplasm, leading to toxicity. In ALS-affected tissues, TDP-43 has been shown to accumulate not only in the cytoplasm but also in mitochondria, causing mitochondrial dysfunction and the release of mitochondrial DNA into the cytoplasm, which activates the innate immune system.

Aberrant accumulation of neurotoxic proteins at the levels of the central nervous system is not only due to their overproduction but also to improper degradation caused mainly by the dysfunction of the two principal protein quality control systems, the ubiquitin-proteasome system (UPS) and the autophagic pathway.

UPS is involved in the degradation of small and short-lived proteins, while autophagy degrades higher dimension proteins and organelles. The most remarkable similarity between the two degradation systems is the labelling of target proteins with ubiquitin to allow the recognition of substrates and facilitate their degradation. Ubiquitination is mediated by a cascade of ubiquitinating enzymes and counter-regulated by deubiquitinating enzymes (DUBs), which can hydrolyse the ubiquitin binding and avoid protein cleavage. Thus, DUBs inhibition stabilizes the ubiquitin bond and promotes degradation, and it is predicted to be beneficial in neurodegenerative diseases like ALS, in which cellular proteostasis is impaired.

In this work, we are specifically interested in DUB USP14. USP14 is a proteosome-associated DUB, which inhibition enhances the UPS, autophagy and mitophagy.

Taking that into account, the specific aims (SA) of this study are:

(SA1) Generating Drosophila lines modelling ALS.

(SA2) Identifying the best concentration of newly available inhibitor of USP14, IU1-366, that enhances proteostasis without affecting flies survival.
(SA3) Addressing potential protective effect of USP14 inhibition in flies modelling ALS.

3. METHODS AND MATERIALS

3.1 Drosophila husbandry and lines generation

Flies were maintained under standard conditions at 23°C on agar cornmeal and yeast food. Control (w^{1118}) and driver lines (*GAL4*) were obtained from Bloomington Drosophila Stock Centre.
Parental lines were already present in the lab stock, so we had to collect virgins and males of the right genotypes and set the crosses.

TABLE 1. Description of parental lines utilized

Name	Description
w^{1118}	Wild-type
$TBPH^{\Delta 23}$/cyoGFP	Deletion of 1616 bp
$TBPH^{1}$/cyoGFP	Entire coding region deletion
UAS-TBPH	Over-expression of TBPH

TABLE 2. Description of drivers utilized

Driver	Expression	Chromosome
da-GAL4	Ubiquitous	III
elav-GAL4	Nervous system	I
tim-GAL4	Clock neurons	II
exex-GAL4	Motor neurons	III
th-GAL4	Dopaminergic neurons	III
d42-GAL4	Motor neurons	III
24b-GAL4	Muscle cells	III

nSyb-GAL4	Nervous system	III
act5c-GAL4	Ubiquitous	II

TABLE 3. MitoQC lines

Crosses	Flies analysed	Description
UAS-mitoQC/cyo-GFP; thGAL4/TM6B x w^{1118}	UAS-mitoQC/+; thGAL4/+	mitoQC expressed in dopaminergic neurons of wild-type adult flies
UAS-mitoQC/cyo-GFP; nSybGAL4/TM6B x w^{1118}	UAS-mitoQC/+; nSybGAL4/+	mitoQC expressed in nervous system of wild-type third instar stage larvae
TBPHΔ23/cyo-GFP; nSybGAL4/TM6B x TBPH1/cyo-GFP, UAS-mitoQC/TM6B	TBPHΔ23/TBPH1; nSybGAL4/UAS-mitoQC	mitoQC expressed in nervous system of TBPHΔ23/TBPH1 third instar stage larvae

3.2 Lifespan

The lifespan assay is a research approach to assess the biology of ageing. We use it to evaluate the effect of different concentrations of the inhibitor IU1-366 on the Drosophila lifetime.

Male flies w^{1118} were collected 12h after their hatching. Food vials were prepared using 0,15g of fly food (Formula 4-24® Instant Drosophila Medium, Plain (Carolina Biological Supply)) to which were added different concentrations of IU1-366 diluted in 600µL of ddH_2O.

Two control groups were used: one with only the culture medium and the other treated with DMSO (dimethyl-sulfoxide).

10 flies were collected for each food vial and passed in new ones every two days. During this transfer, dead flies are counted and annotated.
Two or three independent biological replicates were analysed for each condition considered.

3.3 Climbing activity

The climbing activity assay is a research approach used to study the locomotor function of *Drosophila melanogaster*.
A maximum of 30 male flies between 0 and 3 days post-eclosion were collected. They were introduced into a negative geotaxis counter-current apparatus and given 10 seconds to climb at each position for a total of five attempts. A climbing index score was generated based on the number of flies at each of the positions.
The process was repeated after 20 days on the same flies to understand the effect of ageing on locomotor activity.

3.4 Mitophagy quantification: MitoQC.

3.4.1 Larvae and adult selection

Under normal conditions at 25°C, the larval third instar stage is reached 5-6 days after the cross. Larvae of the right genotype were selected for dissection under the fluorescence microscope. *CyO-GFP* larvae were discarded by checking for GFP fluorescence in the larva, whereas *TM6B* larvae were discarded by checking for the tubby phenotype. Larvae carrying both the *UAS-mitoQC* and the *nSyb-GAL4* were selected for their mCherry fluorescence in the brain.
Adult flies were selected for dissection under the light microscope. *Cyo-GFP* adults were discarded by checking the morphology of wings, curly wing flies were discarded. *TM6B* flies were discarded by checking the number of bristles, flies with a high number of humeral bristles were discarded.

3.4.2 Flies dissection and fixation

L3 larval brain and adult brain were dissected in PBS 1X, pH=7. Brain was fixed with 4% of PFA, pH=7 for 20 minutes. After fixation, it was washed twice in PBS 1X, pH=7.
At the end, the brain was mounted on the slide with 10 µl di Mowiol 4-88 mounting medium (Sigma-Aldrich) and it is covered with a coverslip.
Samples were dissected in the afternoon and imaged the following day.

3.4.3 Immaging and Quantification

Fluorescence microscopy imaging was performed using a Zeiss LSM 900 confocal microscope equipped with 100× and 63x for larval brains and adult brains, respectively. Plan Apochromat (oil immersion, NA 1.4) objective lenses at 2× digital zoom. Z-stacks were acquired at 0.5 µm steps. Two images were taken for each brain. Samples were imaged via sequential excitations (488 nm, green; 561 nm, red). Laser power and gain settings were adjusted depending on the fluorophore but were maintained across samples.
For quantification, maximum intensity projections were created and analysed using Fiji (ImageJ 2.9.0) software. For mitolysosome quantification, the number of mCherry-only puncta was quantified using the mQC-counter plugin, maintaining the same parameters across samples.

3.5 Chymotrypsin-like assay

Extraction was performed from 6 flies for sample. Flies were collected in Eppendorf and frozen in liquid nitrogen. Extraction buffer (Tris 10mM, PH 7.4; EDTA 1mM, Glycerol 20% v/v, ATP 5mM, DTT 5mM) was prepared freshly every time by adding ATP(5mM) and DTT(5mM). Samples were lysed using a pestle and maintained on ice for 30 minutes.
After that, centrifugation was performed at 4°C for 10 minutes. Supernatant, where proteins were present, was collected in a new Eppendorf. Protein concentration was determined by BCA assay according to manufacturer's instructions.

The chymotrypsin-like assay is a luminescent assay that allows to measure the chymotrypsin-like proteolytic activity using a fluorescent substrate.
The substrate used for this assay contains a scissile-quencher-donor pair, that is a covalent chemical bond which can be broken by an enzyme. An increase in the emission from the donor occurs due to the cleavage of the donor-quencher binding performed by the proteasome. This increase can be measured and used to quantify the proteosome activity.
The substrate was prepared by dissolving succinyl-leucine-leucine-valine-tyrosine-amino-luciferin (Suc-LLVY-AMC) in DMSO with a final concentration of 10 mM and then stored at -20°C.
25µg of proteins were charged in each well with proteasome activity buffer (Tris 50Mm, PH 7.4; EDTA 0,5mM) and 1µL of Suc-LLVY-AMC (2 mM, dissolved in DMSO) to a final volume of 200µL.
Plates were incubated at 37°C for 1 hour in the dark and then read at 380 nm excitation and 460 nm emission.
MG132 was used to monitor the specificity; only protein lysate (no substrate) with activity buffer is used to monitor autofluorescence, and only substrate without protein sample to monitor the spontaneous breakdown of the substrate.

3.6 Immunoblot

Extraction was performed from 6 flies for sample. Flies were lysed in RIPA buffer (140 mM NaCl; 65 mM Tris-HCl [pH 7.4]; 1 % NP-40; 0.25 % NaDeoxycholate, 1 mM EDTA, 50mM chloroacetamide, 1x protease Inhibitor Cocktail, 1xPhosSTOP phosphatase inhibitor cocktail).
Samples were lysed using a pestle and maintained on ice for 30 minutes.
After that, centrifugation was performed at 4°C for 10 minutes. Supernatant, where proteins were present, was collected in a new Eppendorf.
Protein concentration was determined by BCA assay according to manufacturer's instructions. 30 µg of proteins were resuspended in 1xLDS with 100 mM DTT and heated for 5 min at 70°C. Equal amounts of protein and volume were loaded and run on 4 %-20 % Bis-Tris ExpressPlus™ PAGE Gels. Gels were transferred via semi-dry Trans Blot Turbo transfer system for 30 min at 25 V onto PVDF membrane for immunoblotting. PVDF membranes were blocked for 1 hour at RT in 5 % milk in TTBS (0.5 M Tris-HCl pH 7.4; 1.5 M NaCl; Tween 20 0.05 %(v/v)) and subsequently

incubated with the total ubiquitin primary antibody diluted (1:500) in TTBS overnight at 4°C. For detection, membranes were washed 3 times for 10 min with TTBS and then incubated 1 h at room temperature with secondary antibodies followed by 3 TTBS washes. Immunoreactivity was detected with Luminata Forte Western HRP substrate and images were acquired using the ImageQuant LAS 4000 instrument. Images from Western Blots were exported and analysed using ImageJ/Fiji.

3.7 Statistical Analysis

Statistical analyses were performed using GraphPad Prism 8 software.
Data are represented as box plots (min to max, all data points showed) or as mean ± SEM. Statistical significance was measured by an unpaired t-test for chymotrypsin-like assay and mitoQC analysis; one-way ANOVA for climbing activity.
Statistical significance is identified as follow: *=p-value ≤ 0,05; **= p-value ≤ 0,01; ***= p-value ≤ 0,001(GraphPad Prism 8 software)

4. RESULTS

4.1 Generation of Drosophila lines modelling ALS

Neurodegenerative diseases, including ALS, have in common the presence of aberrant protein and organelles accumulation, primarily caused by dysfunction in the two major degradative systems of the cell: the ubiquitin-proteasome system (UPS) and autophagy.

USP14, a proteasome-associated deubiquitinating enzyme (DUB), plays a significant role in negatively regulating the UPS and autophagy. Consequently, inhibition of USP14 is expected to enhance the activity of both systems, and it is predicted to be beneficial in models in which organelle and protein homeostasis (proteostasis) is deranged, like ALS.

Remarkably, small-molecule inhibitors of USP14 are commercially available, and can be used for this purpose.

Thus, the principal aim of this study was to test the potential beneficial effect of USP14 inhibition in *in vivo* models of ALS.

To address this aim, we first wanted to generate Drosophila lines modelling *ALS*.

We generated a lack of function model, which proved to be useful to test our hypothesis, and a gain of function model, which did not produce a pathological phenotype suitable for assessing the effects of USP14 inhibition (please see details below).

4.1.1 *TBPH*$^{\Delta 23/1}$ flies show impairment in climbing activity and a decrease in mitophagy levels.

The first model we generated is a loss of function trans-heterozygous combination of the independently derived *TBPH*^{1} and the *TBPH*$^{\Delta 23}$ deletion mutants. TAR DNA-binding protein-43 homolog (*TBPH)* is the orthologue of *TARDBP* in flies.

TBPH$^{\Delta 23/1}$ mutant flies show a strong impairment in climbing activity, which is not present in the control and parental lines (FIGURE 1A).

In this model, we assessed mitophagy levels to investigate whether these mutants show an impairment in organelle homeostasis, and specifically in the degradative pathway underlying mitochondrial quality control.

Mitophagy can be assessed by using MitoQC, a pH-sensitive fluorescent probe containing a tandem GFP-mCherry fusion protein targeted to the outer membrane mitochondrial (OMM) protein FIS1. In normal conditions, both GFP (green) and mCherry (red) fluorescence are visible. During mitophagy, the acidic environment of the lysosome quenches GFP fluorescence, leaving red only puncta, which correspond to mitolysosomes. Ongoing mitophagy can be evaluated by counting the number of mitolysosomes per cell.
Mitophagy levels were detected using the mitoQC fluorescent indicator, which we expressed in the whole nervous systems of the larval brains.
Interestingly, a significant decrease in mitophagy levels was observed in the larval brain of $TBPH^{\Delta 23/1}$ mutants (FIGURE 1B–C).

Thus, $TBPH^{\Delta 23/1}$ flies exhibit a significant impairment in climbing activity and a significant decrease in mitophagy levels. This makes these mutant flies a suitable lack of function model for evaluating the potential beneficial effects of USP14 inhibition.

4.1.2 TBPH overexpression did not produce a pathological phenotype suitable for analysis.

Since overexpression of the *TBPH* gene in Drosophila can also lead to an ALS-like phenotype (Liguori et al., 2021), we overexpressed TBPH in different tissues of the flies to generate a parallel gain of function model.
To induce TBPH expression, we utilized the *UAS-GAL4* system, a yeast-derived method that enables targeted transgene expression in specific tissues. This system comprises two distinct fly lines: one carries the yeast transcription factor *GAL4* under the control of a tissue-specific promoter, while the other contains the transgene positioned downstream of the *UAS* domain, which serves as *GAL4*'s binding site. When these lines are crossed, their progeny (F1) express the transgenic protein exclusively in tissues where *GAL4* is active. (Liguori et al., 2021).
We measured the climbing activity of flies expressing TBPH OE in different tissues at 0 to 3 days post-eclosion. We also aged the flies for 20 days and repeated the climbing test to see if there was any effect due to ageing.
We tested several drivers expressing TBPH in different tissues, but none resulted in impaired climbing activity in either young or aged flies (FIGURE 2). In particular,

we use *da-GAL4*, a ubiquitous expressed driver (FIGURE 2A); *exex-GAL4*, which is expressed in motor neurons (FIGURE 2B), *tim-GAL4*, a clock neurons driver (FIGURE 2C); *elav-GAL4*, which is expressed in the nervous system (FIGURE 2D); *th-GAL4*, that is expressed in dopaminergic neurons (FIGURE 2E) and *d42-GAL4*, which is expressed in motor neurons (FIGURE 2F).

We also tested three additional drivers, which expression resulted in a lethal phenotype: *nSyb-GAL4*, which is expressed in the nervous system, caused lethality after the larval stage; *act5c-GAL4*, a ubiquitous driver, induced lethality at the embryonic stage; *24b-GAL4*, which is expressed in muscle cells, produced smaller larvae that fail to progress to the pupal stage.

In summary, none of the gain of function models that we generated produced a pathological phenotype suitable for assessing the effects of IU1-366 in flies. Gain of function models resulted in either no phenotype or lethality at different stages (larvae, embryos or pupae), which prevented the assessment of IU1-366.

4.2 New inhibitor of USP14, IU1-366, does not affect flies lifespan

Having developed a fly model suitable to address the potential beneficial effect of USP14 inhibition *in vivo*, the next step was to assess the effect of commercially available inhibitors of USP14 in this model.

The development of the first identified USP14 inhibitor, IU1, generated more specific and potent inhibitors such as IU1-47 and, more recently IU1-366, which has never been tested *in vivo*.

With that in mind, we first wanted to determine whether IU1-366 may have any toxic effect on flies.

Thus, to evaluate potential toxicity, we performed a lifespan assay on a wild-type Drosophila line, w^{1118}, by treating flies with increasing concentrations of IU1-366.

The concentration of the inhibitor required to inhibit 50% of the enzymatic activity (IC_{50}) is equal to 63nM. Additionally, since the inhibitor is administered through food, its stability and assimilation by the flies may be affected. Based on these considerations, we decided to feed flies with three different concentrations of IU1-366, and specifically 2µM, 4µM and 10µM.

The lifespan assay indicates that none of the tested inhibitor concentrations affected Drosophila survival, with an average lifespan of approximately 80 days, which is within the typical range for *Drosophila melanogaster* (FIGURE 3).

Thus, we can conclude that IU1-366 does not impact flies' lifespan at any of the tested concentrations and is completely safe.

4.3 Inhibition of USP14 enhances basal mitophagy in adult flies

After confirming that the inhibitor IU1-366 does not affect flies' lifespan at any tested concentration, we aimed to determine whether the IU1-366 treatment is enhancing mitophagy *in vivo*, as this was found to be impaired in the loss of function ALS model that we generated.

We first evaluated the effect of IU1-366 4μM in the larval brain of wild-type flies. The experiment was conducted using a Drosophila wild-type line, which expressed the mitoQC probe specifically in the nervous system.

Mitophagy levels were not altered in larval brains after the treatment with IU1-366 (FIGURE 4A-B).

We next assessed the effect of IU1-366 on mitophagy in the adult fly brain. To do so, we used a Drosophila line, which expressed the mitoQC probe in a small cluster of neurons, and specifically in the dopaminergic neurons.

We treated flies with IU1-366 (4μM/48hrs and 72hrs) and used DMSO as control. After treatment, fly brains were dissected and analysed using a fluorescence microscope Zeiss LSM 900 confocal microscope. For quantification, maximum intensity projections were generated and analysed using Fiji (ImageJ 2.9.0) software. To quantify mitolysosomes, the number of mCherry-only puncta was counted using the mQC-counter plugin.

We detected a significant increase in mitophagy levels in the neurons of adult flies treated with IU1-366 (4μM/72hrs) (FIGURE 4E-F).

In conclusion, inhibition of USP14 with IU1-366 enhances basal mitophagy in the adult brain of wild-type flies.

4.4 IU1-366 does not seem to affect proteasome activity in adult flies.

We next investigated the impact of IU1-366 treatment on the activity of the ubiquitin-proteasome system (UPS), by evaluating the chymotrypsin-like activity of the 20s proteasome core particle.

This protocol outlines a luminescent assay designed to assess the chymotrypsin-like proteolytic activity of the proteasome using a fluorogenic substrate. The substrate incorporates a donor-quencher pair linked by a scissile bond. Upon cleavage by the proteasome, the resulting de-quenching of the donor leads to an increase in fluorescence, which is measured to determine the relative activity of the proteasome.
Experiments were performed on six male wild-type flies per sample, with three replicates performed for each concentration.
Flies were treated for 48 hours or 72 hours with IU1-366 at concentrations of 2µM, 4µM and 10µM, or an equivalent amount of DMSO as a control, administered through food.

We did not detect any changes in the chymotrypsin-like activity upon any of the tested concentrations (FIGURE 5). However, a trend towards an increase in the activity of the UPS was observed after 4µM/48-hour treatment (p-value=0,0784).

4.5 Inhibition of USP14 with IU1-366 does not increase the levels of ubiquitin conjugates.

USP14 contributes to ubiquitin recycling by releasing ubiquitin moieties from chains before proteasomal degradation. Thus, USP14 inhibition may temporarily reduce the pool of free ubiquitin, but in the long term, it leads to accumulation of ubiquitin attached to substrates.
With that in mind, we next evaluated the level of total ubiquitin conjugates as an additional readout of effective USP14 inhibition.
Ubiquitin levels were measured on wild-type flies.
Inhibition of USP14 with IU1-366 (4µM/72hrs) does not seem to affect the level of total ubiquitin conjugates (FIGURE 6).

4.6 Results Figures

Figure 1.

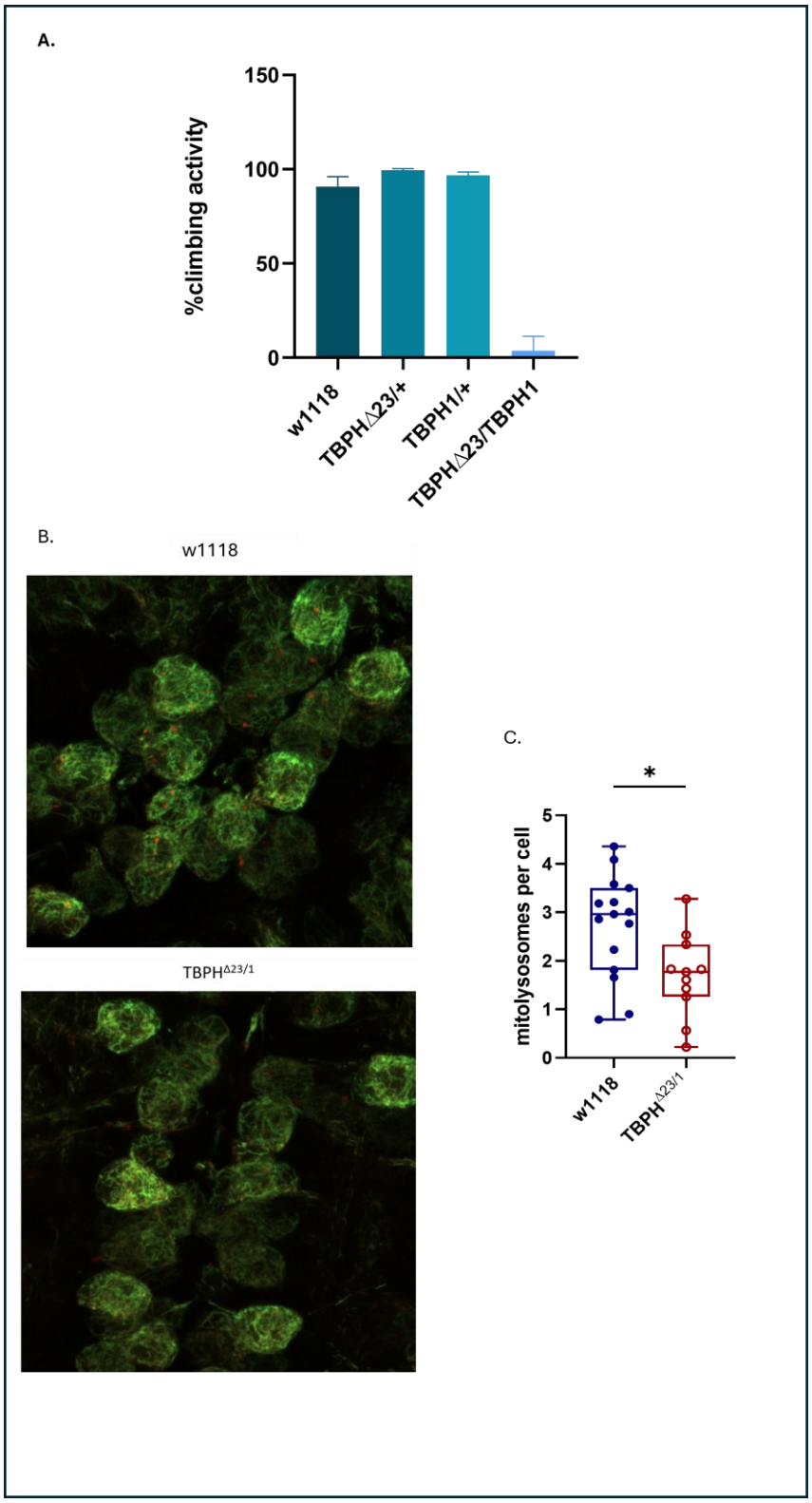

FIGURE 1. *TBPH*$^{\Delta 23/1}$ flies develop impaired climbing activity and a decrease in mitophagy levels. (A) Bar plot showing the percentage of climbing performance of flies. Genotypes analysed were: w^{1118} (control), *TBPH*$^{\Delta 23/+}$ and *TBPH*$^{1/+}$ (flies with single mutation used as control), and *TBPH*$^{\Delta 23/1}$. (B) Representative confocal images of mitolysosomes in larval brain of *TBPH*$^{\Delta 23/1}$ flies and control. mCherry-only puncta represent mitolysosomes (red dots). (C) Quantification of B. Chart shows mean ± SEM of n = 11-15 animals. For each animal, two pictures were taken.

Figure 2.

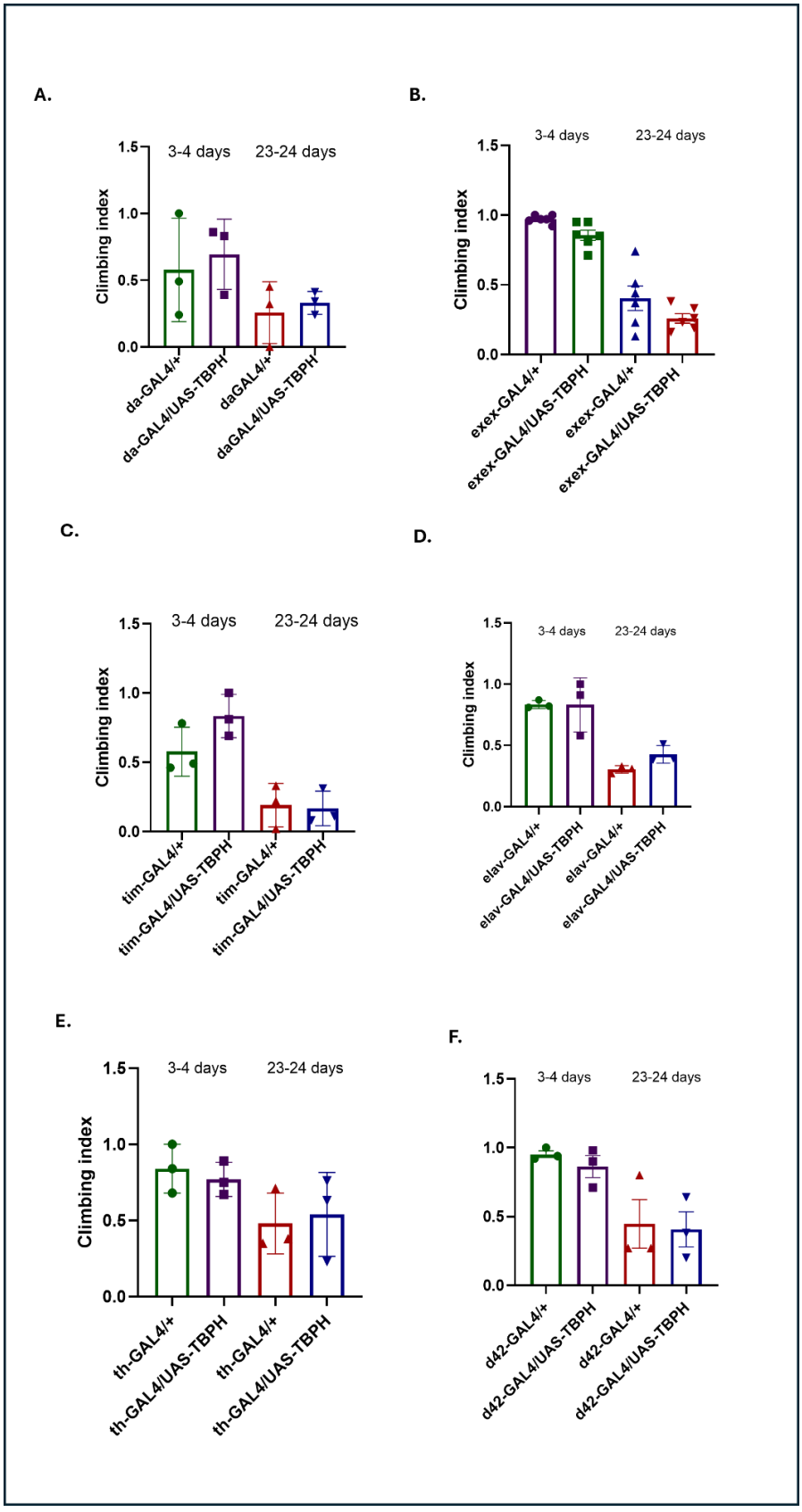
A.
3-4 days
23-24 days
Climbing index
1.5
1.0
0.5
0.0
da-GAL4/+
da-GAL4/UAS-TBPH
daGAL4/+
daGAL4/UAS-TBPH
B.
3-4 days
23-24 days
Climbing index
exex-GAL4/+
exex-GAL4/UAS-TBPH
exex-GAL4/+
exex-GAL4/UAS-TBPH
C.
3-4 days
23-24 days
Climbing index
tim-GAL4/+
tim-GAL4/UAS-TBPH
tim-GAL4/+
tim-GAL4/UAS-TBPH
D.
3-4 days
23-24 days
Climbing index
elav-GAL4/+
elav-GAL4/UAS-TBPH
elav-GAL4/+
elav-GAL4/UAS-TBPH
E.
3-4 days
23-24 days
Climbing index
th-GAL4/+
th-GAL4/UAS-TBPH
th-GAL4/+
th-GAL4/UAS-TBPH
F.
3-4 days
23-24 days
d42-GAL4/+
d42-GAL4/UAS-TBPH
d42-GAL4/+
d42-GAL4/UAS-TBPH

FIGURE 2. No drivers used to induce TBPH overexpression produce an ALS phenotype suitable for analysis. (A) Bar plot showing the percentage of climbing performance of flies. Climbing was performed twice, one with younger flies (3-4 days after eclosion) and one with aged flies (23-24 days after eclosion). Chart shows mean ± SEM of n = 3-6. Genotypes analysed were: *da-GAL4/+, da-GAL4/UAS-TBPH* (A), *exex-GAL4/+, exex-GAL4/UAS-TBPH* (B), *tim-GAL4/+, tim-GAL4/+;UAS-TBPH/+* (C), *elav-GAL4/+;;UAS-TBPH/+*, *elav-GAL4/+;; UAS-TBPH/+* (D), *th-GAL4/+, th-GAL4/UAS-TBPH* (E), *d42-GAL4/+, d42-GAL4/UAS-TBPH* (F

Figure 3

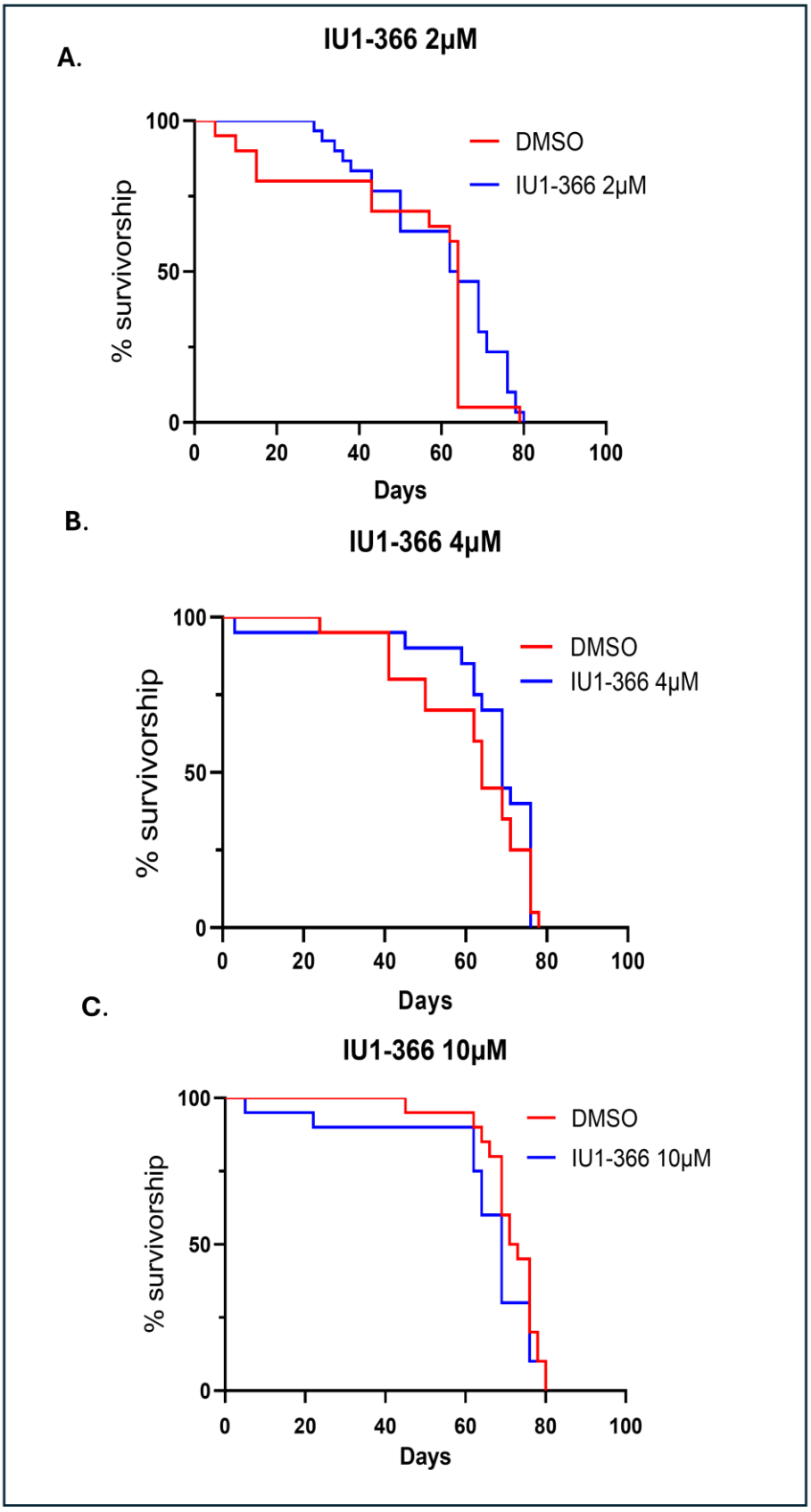
A.
IU1-366 2μM
% survivorship
100
50
0
0
20
40
60
80
100
Days
DMSO
IU1-366 2μM
B.
IU1-366 4μM
% survivorship
100
50
0
0
20
40
60
80
100
Days
DMSO
IU1-366 4μM
C.
IU1-366 10μM
% survivorship
100
50
0
0
20
40
60
80
100
Days
DMSO
IU1-366 10μM

FIGURE 3. The new inhibitor IU1-366 does not affect flies lifespan. Survival plot representing the days of endurance of flies treated with the IU1-366 inhibitor (in blue) at the concentration of 2µM (A), 4µM (B) and 10µM (C) compared to the respective control flies treated with DMSO (in red). n= 30 per genotype.

Figure 4.

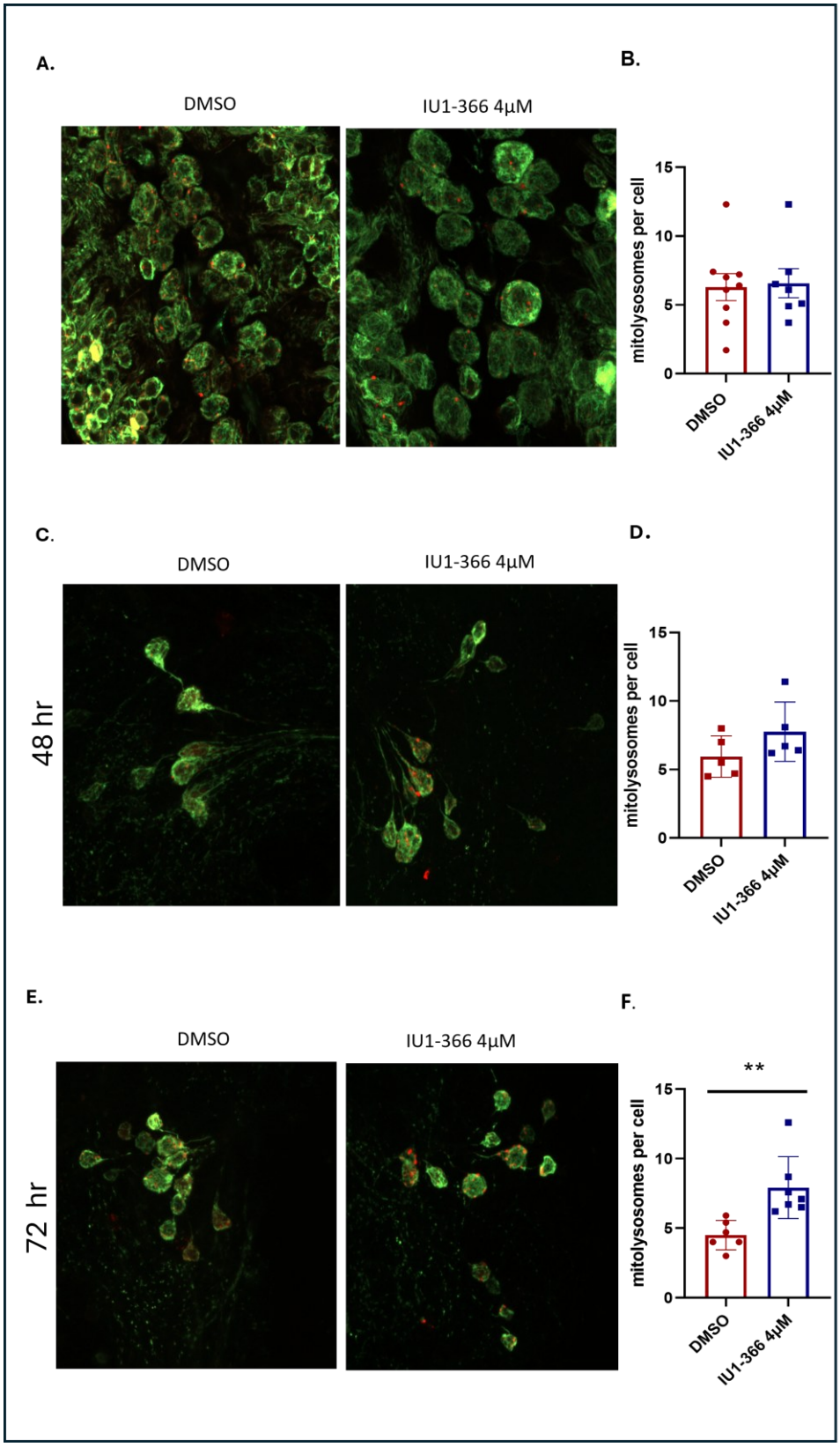
A.
DMSO
IU1-366 4μM
B.
mitolysosomes per cell
15
10
5
0
DMSO
IU1-366 4μM
C.
DMSO
IU1-366 4μM
48 hr
D.
mitolysosomes per cell
15
10
5
0
DMSO
IU1-366 4μM
E.
DMSO
IU1-366 4μM
72 hr
F.
**
mitolysosomes per cell
15
10
5
0
DMSO
IU1-366 4μM

FIGURE 4. Inhibition of USP14 enhances basal mitophagy in adult flies.

Confocal microscopy analysis of Drosophila neurons expressing the mitophagy probe, mitoQC. Images are 3D projections of Z-stacks acquired at the Zeiss LSM 900 confocal microscope. (A) Representative confocal images of mitolysosomes in the larval brain of flies treated with the inhibitor IU1-366 (4μM/48hrs), and relative quantification of mitolysosomes number per cell (B). (C) Representative confocal images of mitolysosomes in dopaminergic neurons of adult flies treated with IU1-366 (4μM/48hrs), and relative quantification of mitolysosomes number per cell (D). (E) Representative confocal images of mitolysosomes in dopaminergic neurons of adult flies treated with IU1-366 (4μM/72hrs) and relative quantification of mitolysosomes number per cell (F). Chart shows mean ± SEM of n = 5-14 animals. For each animal, two pictures were taken. Genotypes analysed were *UAS-mitoQC/+; nSyb-GAL4/+* (control), *UAS-mitoQC/UAS-USP14 RNAi; nSyb-GAL4/+*. UAS-mitoQC/+; nSyb-GAL4/+ were grown in food with the IU1-366 inhibitor.

Figure 5.

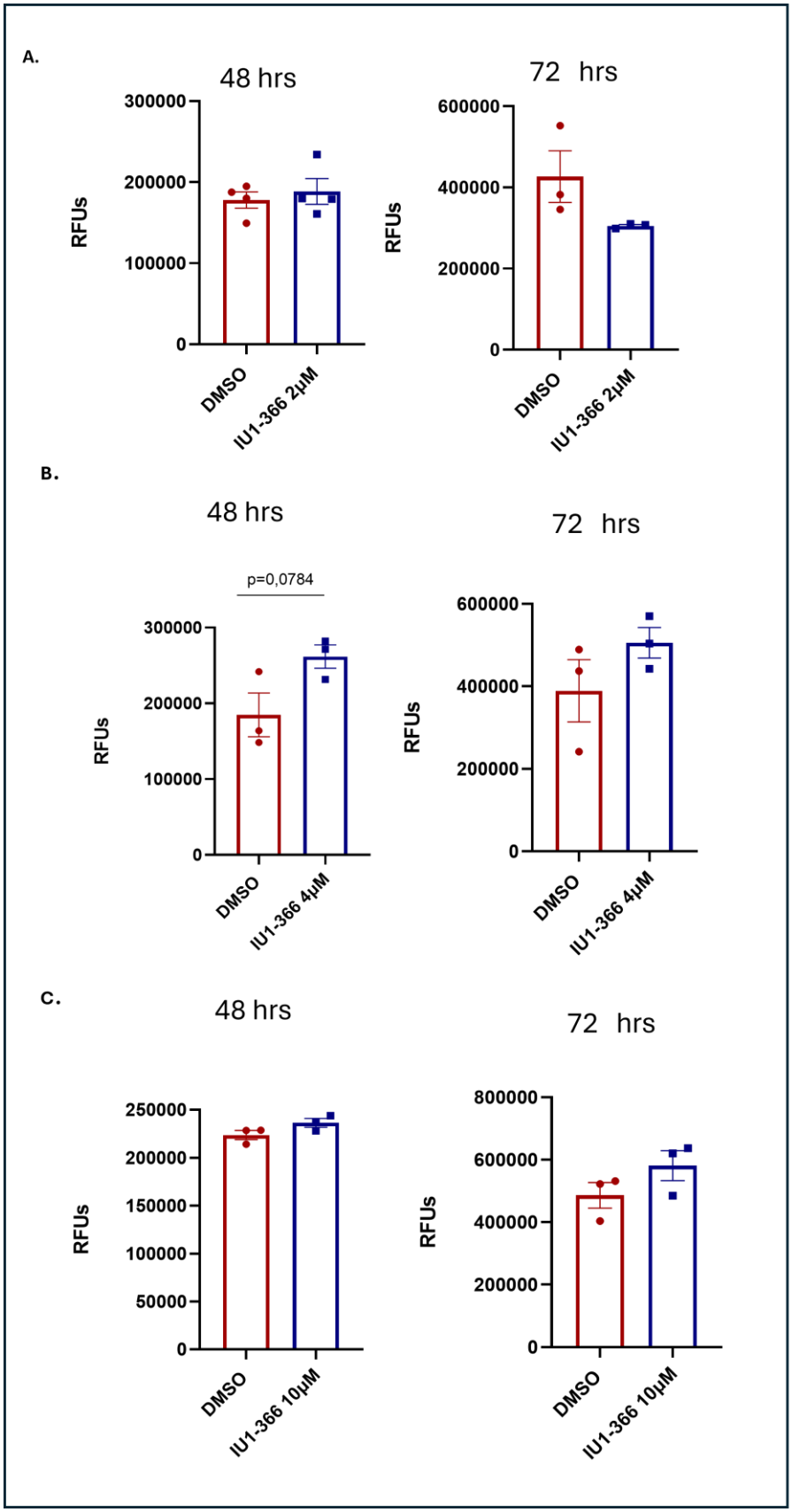
A.
48 hrs
72 hrs
RFUs
300000
200000
100000
0
600000
400000
200000
0
DMSO
IU1-366 2μM
B.
48 hrs
72 hrs
p=0,0784
RFUs
300000
200000
100000
0
600000
400000
200000
0
DMSO
IU1-366 4μM
C.
48 hrs
72 hrs
RFUs
250000
200000
150000
100000
50000
0
800000
600000
400000
200000
0
DMSO
IU1-366 10μM

FIGURE 5. Inhibition of USP14 does not affect proteasome activity of adult flies. (A-C) Bar plot representing the chymotrypsin-like activity of the proteasome in flies treated with increasing concentration (2µM, 4µM and 10µM) of IU1-366 for 4hrs (left panel) or 72hrs (panel on the right). Chart shows mean ± SEM of n=3 replicates

Figure 6

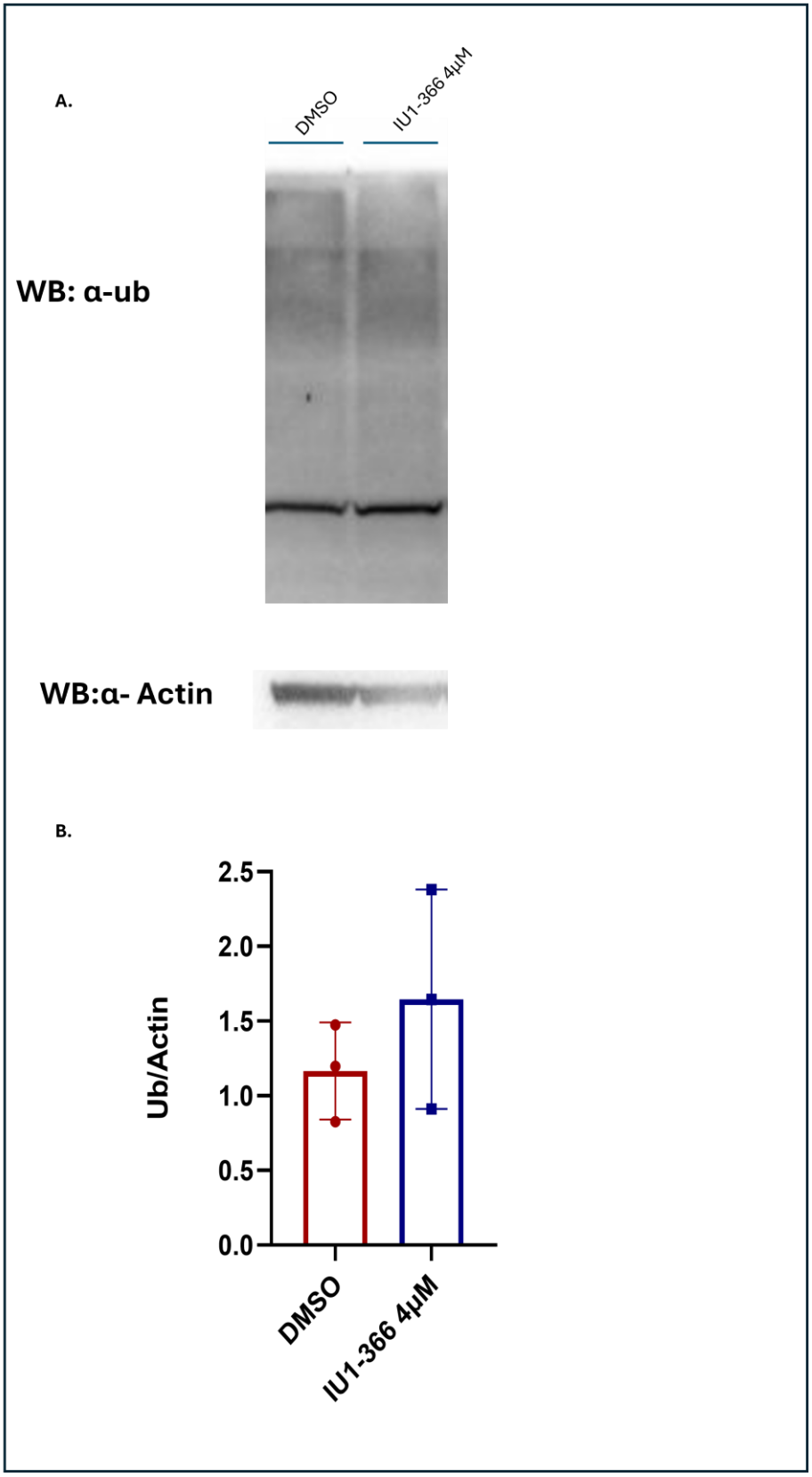
A.
DMSO
IU1-366 4μM
WB: α-ub
WB:α- Actin
B.
Ub/Actin
2.5
2.0
1.5
1.0
0.5
0.0
DMSO
IU1-366 4μM

FIGURE 6. Inhibition of USP14 by IU1-366 does not affect the levels of ubiquitin conjugates.

(A) Western blot analysis of the total ubiquitin conjugates in w^{1118} flies treated with IU1-366 4µM for 72 hours. Actin was used as loading control (B) Data are represented as fold change compared to control conditions. Charts show mean ± SEM. n=3

5. DISCUSSION

Amyotrophic Lateral Sclerosis (ALS) is an adult-onset neurodegenerative disease characterized by the loss of function in motor neurons, including both lower motor neurons at the level of spinal cord and brainstem and upper motor neurons at the level of the motor cortex. Loss of function in these neurons causes muscle weakness, spasticity and atrophy and, in most patients, leads to respiratory failure, which represents the major cause of death.

ALS is a progressive disease and life expectancy is between 2 to 5 years from symptoms onset.

A common phenotype in disease-affected tissue is the formation of toxic aggregates within the cytoplasm, with TDP-43 being the major component. These cytoplasmic aggregates disrupt protein and organelle homeostasis (proteostasis) and trigger cellular stress, thus impairing essential cellular functions.

Alteration in proteostasis and aberrant protein aggregates formation, as seen in ALS, arises not only from excessive protein production but primarily from the dysfunction of key degradative systems of the cell: the ubiquitin-proteasome system (UPS) and autophagy. In this scenario, approaches that enhance the activity of the UPS and autophagy may hold therapeutic promises. Of particular relevance for this project, recent studies have shown that ALS protein TDP-43 also accumulates at the mitochondrial level, leading to organelle dysfunction and the activation of innate immunity processes that presumably contribute to motor neuron impairment and loss (Yu et al., 2020). Thus, enhancement of mitophagy as a means to get rid of dysfunctional mitochondria, sources of oxidative stress and inflammation, can represent a valuable strategy to counteract neurodegeneration in ALS.

A notable similarity between UPS, autophagy and mitophagy is their reliance on ubiquitination to target substrates. Ubiquitination is a reversible process regulated by deubiquitinating enzymes (DUBs), which hydrolyse ubiquitin bonds to prevent protein cleavage. USP14, a proteasome-associated DUB, belongs to the UPS family and plays a crucial role in the negative regulation of both proteasomal and autophagic degradation. Given its function as negative regulator of the two major degradative systems of the cells, inhibition of USP14 represents a potential therapeutic strategy to enhance protein and organelle degradation, restore protein and organelle homeostasis (i.e. proteostasis), and counteract neurodegeneration.

Thus, identifying new inhibitors targeting USP14 is becoming an active field in research, due to the increasing interest in the role of this DUB in the regulation of the degradative systems of the cell, and its involvement as therapeutic target in many pathological conditions.

The first inhibitor of USP14, called IU1, was developed in 2010 by the lab of Dan Finley. (Lee et al., 2010) More specific and more potent inhibitors of USP14 were subsequently developed from the same backbone of IU1. These newly synthetized small molecules, IU1-47 and IU1-366, are extremely appealing tools to counteract neurodegeneration as they appear to be completely benign in murine models, can cross the blood brain barrier (BBB), and exhibit an IC_{50}, which for IU1-366, is in the range of two digits nanomolar.

Notably, a study conducted in our lab demonstrated that the *in vivo* inhibition of USP14 by IU1 restores mitochondrial function and improves locomotor behaviour and lifespan of two Drosophila models of Parkinson's disease. (Chakraborty et al., 2018). The protective effect of USP14 inhibition by IU1 can be ascribed at least in part to the autophagic and mitophagic effect of USP14 inhibition, which we demonstrated in several cellular models (Chakraborty et al., 2018) and more recently in neurons of human origin (Bernardo et al., 2024)

Starting from these evidences, we aim to investigate whether enhancing proteostasis, mitophagy in particular, through USP14 enzymatic inhibition with the new inhibitor IU1-366, can rescue phenotypic deficits in *Drosophila melanogaster* models of ALS. Of note, IU1-366 has never been tested *in vivo* before.

To this aim, we first wanted to generate a reliable fly model of ALS. We generated a loss of function model, in which *TBPH* (*TARDBP* fly orthologue) was deleted ($TBPH^{\Delta 23/1}$). The mutant derives from the crosses of a line with the deletion of an entire coding region, due to insertion and then excision/recombination events ($TBPH^{1}$), and a line with an imprecise excision of a progenitor insertion of about 1616bp, with the complete elimination of the inserted elements ($TBPH^{\Delta 23}$). We performed a climbing assay to assess the level of motor impairment of these flies, and we observed a strong impairment in the climbing activity, with a reduction in the locomotor ability to almost zero. Wild-type flies (w^{1118}) and the parental flies ($TBPH^{1}$ and $TBPH^{\Delta 23}$) were used as control (FIGURE 1A).

In parallel, we measured mitophagy level in the larval brain of these flies, and we observed that the *TBPH*$^{\Delta 23/1}$ flies are characterized by a significant decrease in mitophagy compared to wild type (FIGURE 1B-C).

Having identified a suitable fly model to assess the potential protective effect of USP14 inhibition, we next focused on identifying the concentration of IU1-366 that can induce mitophagy, without resulting in toxicity. To this aim, we examined the lifespan of wild-type flies exposed to three concentrations of IU1-366 (2µM, 4µM, and 10µM), using DMSO-treated flies as control, and no significant differences were observed between inhibitor-treated and control flies, meaning that the inhibitor is not toxic. Importantly, treatment of flies with sub-toxic concentration of IU1-366 (4µM/72hrs) lead to a significant increase in mitophagy in the adult brain (FIGURE 4E-F). The same treatment condition showed a trend towards an increase in proteasome activity (FIGURE 5B). Increasing the number of replicates may conclusively support the hypothesis that USP14 inhibition with IU1-366 effectively enhances both mitophagy and the UPS, thus boosting the proteostatic capability of the cell.

Surprisingly, the identified concentration of IU1-366 that enhanced mitophagy and the UPS, did not affect the levels of total ubiquitin conjugates (FIGURE 6). USP14 plays a crucial role in ubiquitin recycling by cleaving ubiquitin moieties from chains prior to proteasomal degradation. Thus, inhibition of USP14 is expected to result in a reduction of free ubiquitin and, in parallel, an accumulation of ubiquitin-bound substrates, enhancing their detectability in experimental assays. However, we did not detect any effect in the levels of ubiquitin conjugates. Considering the effect that IU1-366 exerts on the UPS and mitophagy, we exclude the possibility that the inhibitor is not working, and we suggest instead that western blotting analysis of ubiquitinated substrates might not be a reliable readout. Indeed, we detected high variability among the samples, suggesting that increasing the number of replicates or changing the approach (i.e. evaluate mRNA levels of ubiquitin genes by qPCR) could help better understand the effect of USP14 inhibition on ubiquitin conjugate levels.

In conclusion, in this work we were able to show that basal mitophagy is impaired in a loss of function model of ALS (TBPH deficient flies) that develop defective motor behaviour and reduced lifespan. We also identified a sub-toxic

concentration of newly available inhibitor of USP14, IU1-366, which proved to induce basal mitophagy in wild type flies. Notably, this is the first time that IU1-366 is tested *in vivo* in flies, and in the context of mitophagy.

Future studies will be conducted to test the effect of IU1-366 in the ALS model that we generated. In particular, we will address whether IU1-366 induces mitophagy in TBPH deficient flies, and if the defective motor behaviour and shorter lifespan of these flies is normalized. Interestingly, preliminary results that we conducted *in vivo* showed that downregulation of USP14 by *RNAi* rescued the lethal phenotype caused by the overexpression of TBPH. As mentioned in the result section, expression of TBPH with nervous system-specific driver *nSyb-GAL4* caused lethality at the larval stage, with larvae that failed to progress into pupae. However, downregulation of USP14 in these flies allowed the progression of larvae into pupae and adult flies. Thus, downregulation of USP14 seems to have counteracted the effect of TBPH overexpression and produced a rescue. Considering this promising result, future experiments will be conducted to evaluate the possible beneficial effect of IU1-366 in flies overexpressing TBPH in the nervous system.

.

6. BIBLIOGRAPHY

A. Prokop-A rough guide to Drosophila mating schemes. (n.d.). https://doi.org/10.6084/m9.figshare.106631

Baldwin, K. R., Godena, V. K., Hewitt, V. L., & Whitworth, A. J. (2016). Axonal transport defects are a common phenotype in *Drosophila* models of ALS. *Human Molecular Genetics*, ddw105. https://doi.org/10.1093/hmg/ddw105

Bernardo, G., Prado, M. A., Dashtmian, A. R., Favaro, M., Mauri, S., Borsetto, A., Marchesan, E., Paulo, J. A., Gygi, S. P., Finley, D. J., & Ziviani, E. (2024). USP14 inhibition enhances Parkin-independent mitophagy in iNeurons. *Pharmacological Research*, *210*, 107484. https://doi.org/10.1016/j.phrs.2024.107484

Chakraborty, J., von Stockum, S., Marchesan, E., Caicci, F., Ferrari, V., Rakovic, A., Klein, C., Antonini, A., Bubacco, L., & Ziviani, E. (2018). USP 14 inhibition corrects an in vivo model of impaired mitophagy . *EMBO Molecular Medicine*, *10*(11). https://doi.org/10.15252/emmm.201809014

Gatica, D., Lahiri, V., & Klionsky, D. J. (2018). Cargo recognition and degradation by selective autophagy. *Nature Cell Biology*, *20*(3), 233–242. https://doi.org/10.1038/s41556-018-0037-z

Gois, A. M., Mendonça, D. M. F., Freire, M. A. M., & Santos, J. R. (2020). IN VITRO AND IN VIVO MODELS OF AMYOTROPHIC LATERAL SCLEROSIS: AN UPDATED OVERVIEW. *Brain Research Bulletin*, *159*, 32–43. https://doi.org/10.1016/j.brainresbull.2020.03.012

Hu, M., Li, P., Song, L., Jeffrey, P. D., Chenova, T. A., Wilkinson, K. D., Cohen, R. E., & Shi, Y. (2005). Structure and mechanisms of the proteasome-associated deubiquitinating enzyme USP14. *EMBO Journal*, *24*(21), 3747–3756. https://doi.org/10.1038/sj.emboj.7600832

Kaushik, S., & Cuervo, A. M. (2015). Proteostasis and aging. In *Nature Medicine* (Vol. 21, Issue 12, pp. 1406–1415). Nature Publishing Group. https://doi.org/10.1038/nm.4001

Kim, H. T., & Goldberg, A. L. (2017). The deubiquitinating enzyme Usp14 allosterically inhibits multiple proteasomal activities and ubiquitin-independent proteolysis. *Journal of Biological Chemistry*, *292*(23), 9830–9839. https://doi.org/10.1074/jbc.M116.763128

Lambert-Smith, I. A., Saunders, D. N., & Yerbury, J. J. (2022). Proteostasis impairment and ALS. In *Progress in Biophysics and Molecular Biology* (Vol. 174, pp. 3–27). Elsevier Ltd. https://doi.org/10.1016/j.pbiomolbio.2022.06.001

Lee, B. H., Lee, M. J., Park, S., Oh, D. C., Elsasser, S., Chen, P. C., Gartner, C., Dimova, N., Hanna, J., Gygi, S. P., Wilson, S. M., King, R. W., & Finley, D. (2010). Enhancement of proteasome activity by a small-molecule inhibitor of USP14. *Nature*, *467*(7312), 179–184. https://doi.org/10.1038/nature09299

Liguori, F., Amadio, S., & Volonté, C. (2021). Fly for ALS: Drosophila modeling on the route to amyotrophic lateral sclerosis modifiers. *Cellular and Molecular Life Sciences*, *78*(17–18), 6143–6160. https://doi.org/10.1007/s00018-021-03905-8

Liu, B., Ruan, J., Chen, M., Li, Z., Manjengwa, G., Schlüter, D., Song, W., & Wang, X. (2022). Deubiquitinating enzymes (DUBs): decipher underlying basis of neurodegenerative diseases. In *Molecular Psychiatry* (Vol. 27, Issue 1, pp. 259–268). Springer Nature. https://doi.org/10.1038/s41380-021-01233-8

Masrori, P., & Van Damme, P. (2020). Amyotrophic lateral sclerosis: a clinical review. *European Journal of Neurology*, *27*(10), 1918–1929. https://doi.org/10.1111/ene.14393

Mejzini, R., Flynn, L. L., Pitout, I. L., Fletcher, S., Wilton, S. D., & Akkari, P. A. (2019). ALS Genetics, Mechanisms, and Therapeutics: Where Are We Now? *Frontiers in Neuroscience*, *13*. https://doi.org/10.3389/fnins.2019.01310

Myeku, N., & Duff, K. E. (2018). Targeting the 26S Proteasome To Protect Against Proteotoxic Diseases. *Trends in Molecular Medicine*, *24*(1), 18–29. https://doi.org/10.1016/j.molmed.2017.11.006

Onishi, M., Yamano, K., Sato, M., Matsuda, N., & Okamoto, K. (2021). Molecular mechanisms and physiological functions of mitophagy. *The EMBO Journal*, *40*(3). https://doi.org/10.15252/embj.2020104705

Robberecht, W., & Philips, T. (2013). The changing scene of amyotrophic lateral sclerosis. In *Nature Reviews Neuroscience* (Vol. 14, Issue 4, pp. 248–264). https://doi.org/10.1038/nrn3430

Scotter, E. L., Chen, H.-J., & Shaw, C. E. (2015). TDP-43 Proteinopathy and ALS: Insights into Disease Mechanisms and Therapeutic Targets. *Neurotherapeutics*, *12*(2), 352–363. https://doi.org/10.1007/s13311-015-0338-x

Snyder, N. A., & Silva, G. M. (2021). Deubiquitinating enzymes (DUBs): Regulation, homeostasis, and oxidative stress response. *Journal of Biological Chemistry*, *297*(3), 101077. https://doi.org/10.1016/j.jbc.2021.101077

Suk, T. R., & Rousseaux, M. W. C. (2020). The role of TDP-43 mislocalization in amyotrophic lateral sclerosis. *Molecular Neurodegeneration*, *15*(1), 45. https://doi.org/10.1186/s13024-020-00397-1

Wang, F., Ning, S., Yu, B., & Wang, Y. (2022). USP14: Structure, Function, and Target Inhibition. In *Frontiers in Pharmacology* (Vol. 12). Frontiers Media S.A. https://doi.org/10.3389/fphar.2021.801328

Wang, X., Hu, Y., & Xu, R. (2024). The pathogenic mechanism of TAR DNA-binding protein 43 (TDP-43) in amyotrophic lateral sclerosis. *Neural Regeneration Research*, *19*(4), 800–806. https://doi.org/10.4103/1673-5374.382233

Wang, Y., Jiang, Y., Ding, S., Li, J., Song, N., Ren, Y., Hong, D., Wu, C., Li, B., Wang, F., He, W., Wang, J., & Mei, Z. (2018). Small molecule inhibitors reveal allosteric regulation

of USP14 via steric blockade. *Cell Research*, *28*(12), 1186–1194. https://doi.org/10.1038/s41422-018-0091-x

Xu, D., Shan, B., Sun, H., Xiao, J., Zhu, K., Xie, X., Li, X., Liang, W., Lu, X., Qian, L., & Yuan, J. (2016). USP14 regulates autophagy by suppressing K63 ubiquitination of Beclin. *Genes and Development*, *30*(15), 1718–1730. https://doi.org/10.1101/gad.285122.116

Yoo, S. M., & Jung, Y. K. (2018). A molecular approach to mitophagy and mitochondrial dynamics. In *Molecules and Cells* (Vol. 41, Issue 1, pp. 18–26). Korean Society for Molecular and Cellular Biology. https://doi.org/10.14348/molcells.2018.2277

Yu, C. H., Davidson, S., Harapas, C. R., Hilton, J. B., Mlodzianoski, M. J., Laohamonthonkul, P., Louis, C., Low, R. R. J., Moecking, J., De Nardo, D., Balka, K. R., Calleja, D. J., Moghaddas, F., Ni, E., McLean, C. A., Samson, A. L., Tyebji, S., Tonkin, C. J., Bye, C. R., … Masters, S. L. (2020). TDP-43 Triggers Mitochondrial DNA Release via mPTP to Activate cGAS/STING in ALS. *Cell*, *183*(3), 636-649.e18. https://doi.org/10.1016/j.cell.2020.09.020